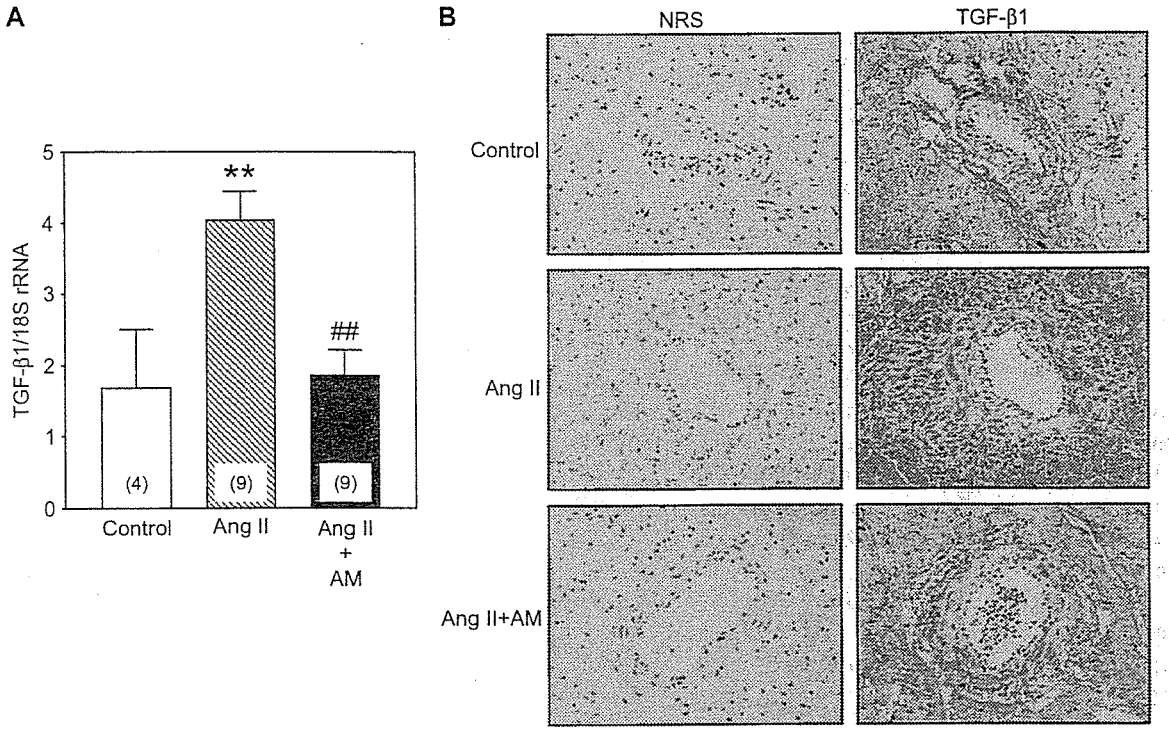

Fig. 4. Effects of Ang II and AM on the gene expression of TGF-β1 in LV (A) and representative pictures for the distribution of TGF-β1 immunoreactivity (B). Values are shown as means±S.E.M. Parentheses indicate the numbers of rats examined and NRS denotes nonimmune rabbit serum. $^{**}p<0.01$, compared to controls; $^{\#\#}p<0.01$, compared to Ang II.

3.5. Plasma levels of rat and human AM

The Ang II infusion had no significant effect on the plasma levels of endogenous rat AM at day 14 (control, 4.7±0.5; Ang II, 5.0±0.3 fmol/mL). Human AM immunoreactivity was detectable only in the plasma of recombinant AM-treated rats at 0.7±0.4 fmol/mL at day 14.

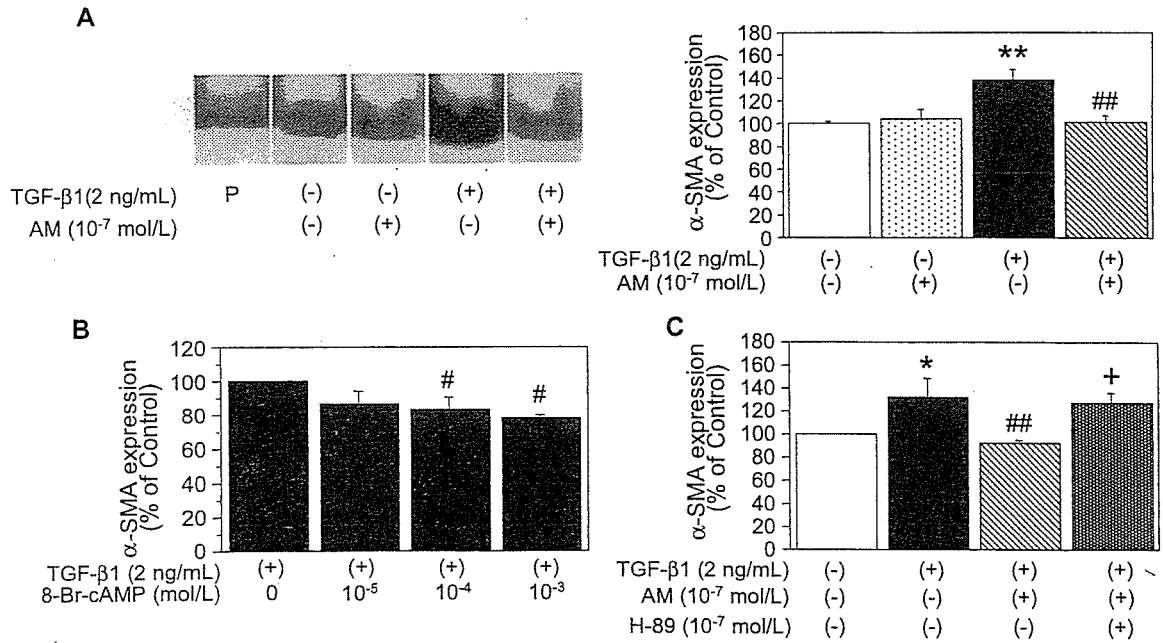

Fig. 5. Effects of AM (A), 8-bromo-cAMP (8-Br-cAMP; B), and H-89, a protein kinase A inhibitor (C) on the α-SMA expression stimulated by TGF-β1 in cultured cardiac fibroblasts. Values are shown as the means±S.E.M. of 5 to 7 (A), 3 (B), and 5 (C) samples examined. $^{*}p<0.05$, $^{**}p<0.01$, compared to controls; $^{\#}p<0.05$, $^{\#\#}p<0.01$ compared to 2 ng/mL TGF-β1; $^{+}p<0.05$, compared to TGF-β1 plus AM. P: human aorta.

3.6. α-SMA expression in vitro

To further clarify the direct action of AM on myofibroblast phenotypic change, cultured cardiac fibroblasts were treated with TGF-β1 and/or AM to look at the expression level of α-SMA. Fig. 5A illustrates a representative Western blot and the composite data. Two ng/mL TGF-β1 significantly ($p<0.01$) increased the α-SMA expression by 38% in these cells. Treatment with 10^{-7} mol/L AM significantly ($p<0.01$) inhibited the TGF-β1-induced α-SMA expression by 27%. Similarly, 8-bromo-cAMP, an analogue of cyclic AMP (cAMP), inhibited the α-SMA expression induced by TGF-β1 (Fig. 5B); while pretreatment with 10^{-7} mol/L H-89, a specific protein kinase A inhibitor, significantly ($p<0.05$) attenuated the action of AM (Fig. 5C).

4. Discussion

In this study, we report that AM attenuates the Ang II-induced perivascular fibrosis of coronary arteries, suppressing myofibroblast differentiation and expressions of TGF-β1 and type 1 collagen, without affecting blood pressure, left ventricular weight, and cross-sectional area of myocardial fiber. Ventricular remodeling characterized by *myocardial* hypertrophy and fibrosis results in serious consequences for cardiac function. Remodeling of the myocardium involves alteration of the function of fibroblasts, the major cells making up two-thirds of the total cell number in the heart [22]. Fibroblasts change their phenotype to myofibroblasts capable of producing ECM proteins, and this was reported to be a critical step for progression of the fibrosis [3]. The ECM initially accumulates around coronary arteries in response to systemic hypertension and then expands into the interstitial space between *myocardial fibers* [2], therefore suppressing the activation of perivascular fibroblasts might be important to attenuate the adverse remodeling. Using an Ang II-induced hypertensive model, our study supports the previous report by Campbell et al. [7] that Ang II temporally induces the phenotypic change of fibroblasts in the rat heart.

We previously showed that synthetic AM inhibited the Ang II-induced cellular proliferation and growth of cultured cardiac fibroblasts [13]. Consistent with our previous in vitro study [13], we observed in the present study that AM exerted an antiproliferative effect on fibroblasts as determined by the number of Ki-67-positive cells, counteracting the effect of Ang II. In addition, we demonstrated for the first time that the number of adventitial fibroblasts expressing α-SMA, a marker for fibroblast activation, significantly decreased following the AM administration. It should be noted that these AM effects were observed with little change in blood pressure and in left ventricle/body weight and *size of myocardial fiber*. Accordant with the in vitro study by Tomoda et al. [23], cardiac fibroblasts may be more sensitive to AM than *cardiocytes*. Meanwhile, we recently reported using a rat model of myocardial infarction, that AM infusion in an acute phase of the infarction inhibited not only chronic progression of interstitial fibrosis but also of *myocardial* hypertrophy [15]. This seems inconsistent with the present study in terms of alleviation of cardiac hypertrophy; however, the model differs from each other and left ventricular end-diastolic pressure was lowered by the AM infusion in our myocardial infarction experiment. This difference may support the hypothesis for differential regulation of *myocardial* hypertrophy and fibrosis; inappropriate humoral activations stimulate myocardial fibrosis, while hemodynamic factors regulate *growth of myocardial fibers* [2,10,24]. Another possible explanation for the inconsistency may be a difference in the experimental periods of 2 vs. 9 weeks. Because humoral factors including endothelin-1 and TGF-β1 produced by cardiac fibroblasts have been reported to be involved in the *cardiocyte* growth in vitro [25,26], AM treatment for longer periods of time would reduce *growth of myocardial fibers* by modulating fibroblast function.

TGF-β1 plays an important role in myocardial and vascular fibrosis by stimulating the phenotypic change of fibroblasts to myofibroblasts [3] capable of producing matrix proteins. Indeed, blockage of the TGF-β1 action produced the beneficial effect on fibrosis in pressure-overloaded heart [10]. This is comparable with the report by Jesmin et al. [27] showing that the TGF-β1 immunoreactivity is intensely stained in the perivascular area as well as in the vascular wall, concomitantly with TGF-β1 gene up-regulation, in the process of vascular remodeling. In the present study, the reductions of TGF-β1 and type 1 collagen expression with reduced collagen deposition were observed in the AM-treated rats. Both TGF-β1 and AM have been reported to be expressed in a similar pattern during the development of embryonic mouse heart [28] and, in addition, von der Hardt et al. [29] reported that aerosolized AM inhibited TGF-β1 gene expression in the porcine lung. Thus, there seems to be interaction between these two growth-regulatory factors in the process of vascular remodeling.

Many of the AM actions have been shown to be mediated by accumulation of intracellular cyclic AMP (cAMP) [12] and consistent with this, significance of cAMP signaling in attenuating the myofibroblastic change was reported in lung fibroblasts [30] and in hepatic stellate cells [31]. Our in vitro experiments of this study showed that both AM and the cAMP analogue inhibited protein expression of α-SMA induced by TGF-β1 in cultured cardiac fibroblasts; while the protein kinase A inhibition reversed the action of AM. In comparison with the in vivo experiments, the much higher concentration of AM was required to see the clear suppression of α-SMA levels in cultured cardiac fibroblasts; although the present findings suggest possible involvement of the cAMP-protein kinase A pathway in attenuation of the myofibroblast differentiation by AM.

According to the recent reports, heterozygotes of AM knockout mice have shown augmented responses of interstitial or perivascular fibrosis in the myocardium of pressure overload [32] and Ang II/salt-loading hypertension [33] and of intimal hyperplasia in cuff-induced vascular injury [34], compared to their littermates, suggesting cardiovascular protective effects of AM. The proposed mechanisms for such AM effects protective against cardiovascular remodeling are suppression of the renin–angiotensin–aldosterone system and reductions of oxidative stress and protein kinase C activity [15,32–34]. Our present study suggests the profile of AM as an antifibrotic factor counteracting TGF-β1 action by modulating myofibroblast differentiation in the process of vascular remodeling. Meanwhile, Ang II was used to induce hypertension and coronary perivascular fibrosis in the present study, but we are unable to attribute the beneficial effects of AM to specific inhibition of the action of Ang II. These effects may be expected in other forms of hypertension; although further studies are necessary to clarify this point.

In summary, AM infusion for 2 weeks attenuated the Ang II-induced coronary matrix remodeling, suppressing fibroblast activation and expression of TGF-β1 in rats. Because AM is produced in the myocardium and vascular wall, these findings further support the notion that AM is a modulator of cardiovascular remodeling via modulation of fibroblast function.

Acknowledgements

This study was supported by the grants-in-aid for Scientific Research on Priority Areas and for the 21st Century Centers of Excellence Program (Life Science) from the Ministry of Education, Culture, Sport, Science and Technology, Japan, and by a grant-in-aid from AstraZeneca Research 2003. We gratefully thank Ms. Ritsuko Sotomura and Mariko Tokashiki for their technical assistance.

References

[1] Weber KT. Targeting pathological remodeling: concepts of cardioprotection and reparation. Circulation 2000;102:1342–5.
[2] Nicoletti A, Michel JB. Cardiac fibrosis and inflammation: interaction with hemodynamic and hormonal factors. Cardiovasc Res 1999; 41:532–43.
[3] Powell DW, Mifflin RC, Valentich JD, Crowe SE, Saada JI, West AB. Myofibroblasts: I. Paracrine cells important in health and disease. Am J Physiol 1999;277(Cell Physiol 46):C1–9.
[4] Shi Y, O'Brien JE Jr, Fard A, Zalewski A. Transforming growth factor-β1 expression and myofibroblast formation during arterial repair. Arterioscler Thromb Vasc Biol 1996;16:1298–305.
[5] Campbell SE, Katwa LC. Angiotensin II stimulated expression of transforming growth factor-β1 in cardiac fibroblasts and myofibroblasts. J Mol Cell Cardiol 1997;29:1947–58.
[6] McEwan PE, Gray GA, Sherry L, Webb DJ, Kenyon CJ. Differential effects of angiotensin II on cardiac cell proliferation and intramyocardial perivascular fibrosis in vivo. Circulation 1998; 98:2765–73.
[7] Campbell SE, Janicki JS, Weber KT. Temporal differences in fibroblast proliferation and phenotype expression in response to chronic administration of angiotensin II or aldosterone. J Mol Cell Cardiol 1995;27:1545–60.
[8] Lijnen PJ, Petrov VV, Fagard RH. Association between transforming growth factor-β and hypertension. Am J Hypertens 2003;16:604–11.
[9] Wilcox JN, Okamoto EI, Nakahara KI, Vinten-Johansen J. Perivascular responses after angioplasty which may contribute to postangioplasty restenosis: a role for circulating myofibroblast precursors? Ann N Y Acad Sci 2001;947:68–90.
[10] Kuwahara F, Kai H, Tokuda K, Kai M, Takeshita A, Egashira K, et al. Transforming growth factor-β function blocking prevents myocardial fibrosis and diastolic dysfunction in pressure-overloaded rats. Circulation 2002;106:130–5.
[11] Kitamura K, Kangawa K, Kawamoto M, Ichiki Y, Nakamura S, Matsuo H, et al. Adrenomedullin: a novel hypotensive peptide isolated from human pheochromocytoma. Biochem Biophys Res Commun 1993;192:553–60.
[12] Kitamura K, Kangawa K, Eto T. Adrenomedullin and PAMP: discovery, structures, and cardiovascular functions. Microsc Res Tech 2002;57:3–13.
[13] Tsuruda T, Kato J, Kitamura K, Kawamoto M, Kuwasako K, Imamura T, et al. An autocrine or a paracrine role of adrenomedullin in modulating cardiac fibroblast growth. Cardiovasc Res 1999;43:958–67.
[14] Horio T, Nishikimi T, Yoshihara F, Matsuo H, Takishita S, Kangawa K. Effects of adrenomedullin on cultured rat cardiac myocytes and fibroblasts. Eur J Pharmacol 1999;382:1–9.
[15] Nakamura R, Kato J, Kitamura K, Onitsuka H, Imamura T, Cao Y, et al. Adrenomedullin administration immediately after myocardial infarction ameliorates progression of heart failure in rats. Circulation 2004;110:426–31.
[16] Tsuruda T, Jougasaki M, Boerrigter G, Costello-Boerrigter LC, Cataliotti A, Lee SC, et al. Ventricular adrenomedullin is associated with myocyte hypertrophy in human transplanted heart. Regul Pept 2003;112:161–6.
[17] Tsuruda T, Kato J, Kitamura K, Imamura T, Koiwaya Y, Kangawa K, et al. Enhanced adrenomedullin production by mechanical stretching in cultured rat cardiomyocytes. Hypertension 2000;35:1210–4.
[18] Ota T, Takamura T, Ando H, Nohara E, Yamashita H, Kobayashi K. Preventive effect of cerivastatin on diabetic nephropathy through suppression of glomerular macrophage recruitment in a rat model. Diabetologia 2003;46:843–51.
[19] Nishikawa N, Yamamoto K, Sakata Y, Mano T, Yoshida J, Miwa T, et al. Differential activation of matrix metalloproteinases in heart failure with and without ventricular dilatation. Cardiovasc Res 2003;57:766–74.
[20] Proudnikov D, Yuferov V, Zhou Y, LaForge KS, Ho A, Kreek MJ. Optimizing primer-probe design for fluorescent PCR. J Neurosci Methods 2003;123:31–45.
[21] Tsuruda T, Boerrigter G, Huntley BK, Noser JA, Cataliotti A, Costello-Boerrigter LC, et al. Brain natriuretic peptide is produced in cardiac fibroblasts and induces matrix metalloproteinases. Circ Res 2002;91:1127–34.
[22] Zak R. Cell proliferation during cardiac growth. Am J Cardiol 1973;31:211–9.
[23] Tomoda Y, Kikumoto K, Isumi Y, Katafuchi T, Tanaka A, Kangawa K, et al. Cardiac fibroblasts are major production and target cells of adrenomedullin in the heart in vitro. Cardiovasc Res 2001;49:721–30.
[24] Burlew BS, Weber KT. Connective tissue and the heart. Functional significance and regulatory mechanisms. Cardiol Clin 2000; 18:435–42.
[25] Gray MO, Long CS, Kalinyak JE, Li HT, Karliner JS. Angiotensin II stimulates cardiac myocyte hypertrophy via paracrine release of

TGF-β1 and endothelin-1 from fibroblasts. Cardiovasc Res 1998;40: 352–63.

[26] Harada M, Saito Y, Nakagawa O, Miyamoto Y, Ishikawa M, Kuwahara K, et al. Role of cardiac nonmyocytes in cyclic mechanical stretch-induced myocyte hypertrophy. Heart Vessels 1997;12:198–200.

[27] Jesmin S, Sakuma I, Hattori Y, Kitabatake A. Role of angiotensin II in altered expression of molecules responsible for coronary matrix remodeling in insulin-resistant diabetic rats. Arterioscler Thromb Vasc Biol 2003;23:2021–6.

[28] Montuenga LM, Mariano JM, Prentice MA, Cuttitta F, Jakowlew SB. Coordinate expression of transforming growth factor-β1 and adrenomedullin in rodent embryogenesis. Endocrinology 1998;139:3946–57.

[29] von der Hardt K, Kandler MA, Popp K, Schoof E, Chada M, Rascher W, et al. Aerosolized adrenomedullin suppresses pulmonary transforming growth factor-β1 and interleukin-1β gene expression in vivo. Eur J Pharmacol 2002;457:71–6.

[30] Kolodsick JE, Peters-Golden M, Larios J, Toews GB, Thannickal VJ, Moore BB. Prostaglandin E_2 inhibits fibroblast to myofibroblast transition via E. prostanoid receptor 2 signaling and cyclic adenosine monophosphate elevation. Am J Respir Cell Mol Biol 2003;29:537–44.

[31] Mallat A, Préaux AM, Serradeil-Le Gal C, Raufaste D, Gallois C, Brenner DA, et al. Growth inhibitory properties of endothelin-1 in activated human hepatic stellate cells: a cyclic adenosine monophosphate-mediated pathway. Inhibition of both extracellular signal-regulated kinase and c-Jun kinase and upregulation of endothelin B receptors. J Clin Invest 1996;98:2771–8.

[32] Niu P, Shindo T, Iwata H, Iimuro S, Takeda N, Zhang Y, et al. Protective effects of endogenous adrenomedullin on cardiac hypertrophy, fibrosis, and renal damage. Circulation 2004;109:1789–94.

[33] Shimosawa T, Shibagaki Y, Ishibashi K, Kitamura K, Kangawa K, Kato S, et al. Adrenomedullin, an endogenous peptide, counteracts cardiovascular damage. Circulation 2002;105:106–11.

[34] Kawai J, Ando K, Tojo A, Shimosawa T, Takahashi K, Onozato ML, et al. Endogenous adrenomedullin protects against vascular response to injury in mice. Circulation 2004;109:1147–53.

Available online at www.sciencedirect.com

SCIENCE DIRECT®

European Journal of Pharmacology 508 (2005) 201–204

ejp

www.elsevier.com/locate/ejphar

Adrenomedullin alleviates not only neointimal formation but also perivascular hyperplasia following arterial injury in rats

Toshihiro Tsuruda[a,b,*], Johji Kato[a], Eizaburo Matsui[a], Kinta Hatakeyama[c], Hiroyuki Masuyama[a], Takuroh Imamura[a], Kazuo Kitamura[a], Yujiro Asada[c], Tanenao Eto[a]

[a]*First Department of Internal Medicine, Miyazaki Medical College, University of Miyazaki, Japan*
[b]*Department of Nutrition Management, Faculty of Health and Nutrition, Minami-Kyushu University, Japan*
[c]*First Department of Pathology, Miyazaki Medical College, University of Miyazaki, Japan*

Received 19 August 2004; received in revised form 11 November 2004; accepted 10 December 2004
Available online 7 January 2005

Abstract

Producing components of the extracellular matrix, the vascular adventitia has been recognized as an important modulator of the vascular remodeling process, which determines the vessel architecture. In this study, we examined the effect of the vasodilator peptide adrenomedullin on vascular remodeling induced by balloon injury of rat carotid arteries. Endothelial denudation with wall stretch by ballooning not only induced neointimal formation accompanied with a reduced ratio of the lumen to vessel area, but also increased the fibroblast number and collagen deposition in the adventitial layer. When compared with the saline infusion, intravenous adrenomedullin infusion at 200 ng/h for 14 days suppressed the neointimal formation (−33%, P=0.033), reversing the ratio of lumen to vessel ratio (P=0.030), without affecting systolic blood pressure. Moreover, the adrenomedullin infusion decreased the number of adventitial fibroblasts (−41%, P<0.001) and the collagen deposition (−36%, P=0.006) in the adventitial layer of the injured artery. In conclusion, the intravenous adrenomedullin infusion effectively attenuates vascular remodeling following the arterial injury via suppression of hyperplasia in the intima and adventitia, suggesting a potential of adrenomedullin as a therapeutic tool against vascular remodeling.

Keywords: Remodeling; Extracellular matrix; Adventitia

1. Introduction

Arterial remodeling is a physiological and pathological reaction in response to hemodynamic, immunologic, and biochemical stimuli (Pasterkamp et al., 2004). Medial hypertrophy and neointimal lesion were focused on as important features; however recent studies have concentrated on reorganization of the entire vessel architecture as vascular remodeling (Strauss and Rabinovitch, 2000; Ward et al., 2000). Accumulating evidence suggests an importance for the adventitial layer, which modulate the remodeling process through regulation of the extracellular matrix formation (Sartore et al., 2001; Strauss and Rabinovitch, 2000). A rodent model of arterial balloon injury is widely used to examine the remodeling process due to its similarity to restenotic vascular lesions seen after angioplasty in humans (De Meyer and Bult, 1997). In this model, the vascular injuries cause proliferation and migration of vascular smooth muscle cells (VSMC) into the intima, and fibroblasts increase in cell number, along with an increase in extracellular matrix deposition in the adventitial layer, further aggravating vascular remodeling (Sartore et al., 2001; Ryan et al., 2003). Various humoral interactions between growth factors, inflammatory cytokines or vasoactive peptides have been reported to be involved in the remodeling process (Sartore et al., 2001). Adrenomedullin, initially isolated from human pheochromocytoma (Kitamura et al., 1993), has been shown to have multiple functions in the cardiovascular system (Kitamura

* Corresponding author. First Department of Internal Medicine, Miyazaki Medical College, University of Miyazaki, 5200 Kihara Kiyotake, Miyazaki 889-1692, Japan. Tel.: +81 985 85 0872; fax: +81 985 85 6596.
E-mail address: ttsuruda@med.miyazaki-u.ac.jp (T. Tsuruda).

0014-2999/$ - see front matter © 2004 Elsevier B.V. All rights reserved.
doi:10.1016/j.ejphar.2004.12.019

et al., 2002). Adrenomedullin was shown to inhibit the migration and proliferation of VSMC in vitro (Kano et al., 1996; Kohno et al., 1997), and Agata et al. (2003) reported that adrenomedullin gene delivery produced an inhibitory action on neointima formation after balloon injury, suggesting an important role for this bioactive peptide in vascular remodeling. However, it remains unknown whether the adrenomedullin actions are observed only in the vascular intimal layer or in the whole vascular structure in the remodeling process. The aim of the present study was to examine the biological actions of adrenomedullin on vascular remodeling, which includes not only the neointima formation but also the adventitia hyperplasia in balloon-injured carotid arteries of rats.

2. Materials and methods

The present study was performed in accordance with the Animal Welfare Act and with approval of the University of Miyazaki Institutional Animal Care and Use Committee (2003-023).

2.1. Experimental protocol

Ten- to eleven-week-old male Sprague-Dawley rats (CLEA, Japan, Inc.) weighing 350–400 g were housed in a temperature- and light-controlled room (25±1 °C; 12/12-h light/dark cycle) with normal rat chow and water given ad libitum. After the rats were anesthetized with 40 mg/kg i.p. of pentobarbital sodium, endothelial denudation and wall stretch of the left common carotid artery were carried out by three passages of a Fogarty 2F balloon catheter (Baxter International, Deerfield, IL, USA). Then, the rats were randomly divided into two groups infused with saline (n=9) or with synthetic rat adrenomedullin (Peptide Institute, Osaka, Japan) at 200 ng/h (n=6) over 14 days. Immediately after the balloon injury, miniosmotic pumps (Alzet model 2002) were implanted subcutaneously to release either saline or adrenomedullin into the right external jugular vein. Blood pressure was monitored by tail-cuff plethysmography during the experimental period. At day 14, the rats were anesthetized with 40 mg/kg i.p. of pentobarbital sodium and blood samples were collected from the inferior vena cava. Both the injured left common carotid artery and non-injured contralateral were perfused via the left ventricle with phosphate buffer-saline, followed by perfusion fixation with 4% paraformaldehyde, at the physiological constant pressure of about 100 mm Hg, and were then immediately excised.

2.2. Histology and morphological evaluation

The carotid arteries embedded in paraffin were sectioned at 2 μm thickness. After deparaffinization with xylene and graded alcohol, slides were incubated with 0.1% picrosirius red (Direct Red 80, Sigma) dissolved in saturated picric acid for 10 min. Morphological evaluation of the injured and contralateral uninjured carotid arteries was performed at the middle portion of the artery by a single observer in a blind manner. Two samples were too disfigured to be precisely quantified: one was an injured artery of the control and the other was an intact artery of the adrenomedullin group. Therefore, these two samples were excluded from the analysis. The cross-sectional areas of the lumen and those circumscribed by the internal or external elastic lamina were determined by computerized measurement (Axio Vison 2.05 Carl ZEISS, Munchen, Germany), and the areas of the media and intima were calculated by subtraction. The vessel area was defined as the area surrounded by the external elastic lamina. The number of fibroblasts showing a typical spindle shape in the adventitia was determined at a magnification of ×400. To quantify collagen deposition in the vascular wall, sections stained with picrosirius red were scanned by Mac Scope (v. 2.3.2) software under polarized light. The tightly packed collagen surrounding the carotid artery was defined as the collagen deposition in this study.

2.3. Assay for adrenomedullin

Plasma concentrations of rat adrenomedullin were measured with a specific radioimmunoassay, which detects the C-terminal amide structure of adrenomedullin, an essential portion for the biological activity, as previously described (Tsuruda et al., 1999).

2.4. Statistical analysis

All data are expressed as means±S.E.M. Comparisons between groups were made with one-way analysis of variance followed by the Fisher's test, and statistical significance was accepted at $P<0.05$.

3. Results

3.1. Plasma level of rat adrenomedullin and blood pressure

The adrenomedullin-supplemented rats showed significantly higher rat adrenomedullin levels in the plasma compared with those administered with saline at day 14 (adrenomedullin group, 4.9±0.5; saline group, 3.3±0.2 fmol/ml; P=0.004). Meanwhile, no significant difference in systolic blood pressure was noted before and during the experiment period (data not shown).

3.2. Effects adrenomedullin on neointimal formation and adventitia hyperplasia

Fig. 1 illustrates the hematoxylin-eosin stainings of the intact and balloon-injured carotid arteries at day 14. In the injured artery (B), neointima formation occurred and the

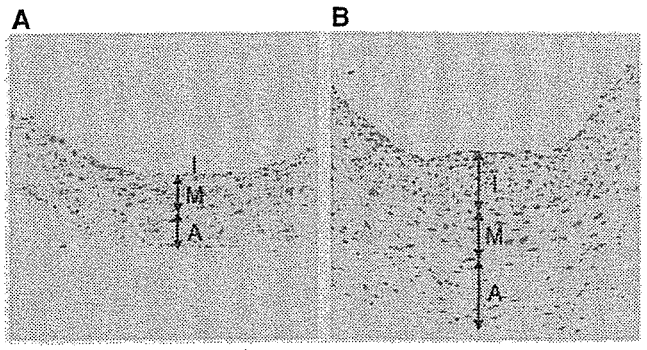

Fig. 1. Histological findings of the intact (A) and injured (B) arteries. I, intima; M, media; A, adventitia. Original magnification, ×200.

adventitial layer thickened with high cellularity, compared with the intact artery (A).

In the quantitative analysis (Fig. 2), the injured arteries showed significant neointimal formation ($P<0.001$) with little influence on the medial area (A) resulting in a significant increase of the intima to media ratio (B). As shown, the adrenomedullin infusion for 14 days significantly attenuated the neointimal formation by 33% ($P=0.033$) and the intima to media ratio by 34% ($P=0.025$), respectively, compared with the saline infusion, while adrenomedullin had no effect on these parameters in the contralateral, intact artery.

Fig. 3A illustrates the effect of adrenomedullin on cell number of fibroblasts in the adventitial layer. The arterial injury increased the number of fibroblasts ($P<0.001$), but this increase was suppressed by the adrenomedullin infusion by 41% ($P<0.001$). Fig. 3B shows the effect of adrenomedullin on the ratio of collagen deposition to the medial areas in the intact and injured arteries. The balloon injury enlarged the collagen deposition area mainly in the adventitia ($P<0.001$); however, the adrenomedullin infusion reduced it by 38% ($P=0.006$).

3.3. Effect of adrenomedullin on geometrical changes in the carotid arteries

Fig. 4A and B illustrate the effect of adrenomedullin on the lumen and vessel areas, respectively. The balloon injury slightly reduced the lumen area of rats infused with saline,

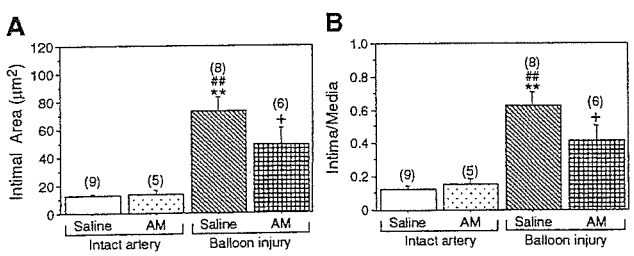

Fig. 2. Effect of adrenomedullin on intimal area (A) and ratio of intima to media (B) in the intact and injured arteries. Values are means±S.E.M., (n). $^{**}P<0.01$ vs. intact artery with saline infusion; $^{\#\#}P<0.01$ vs. intact artery with adrenomedullin infusion; $^{+}P<0.05$ vs. injured artery with saline infusion.

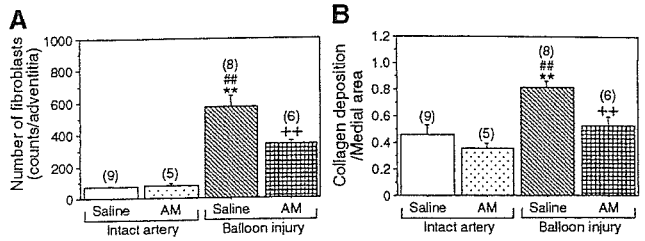

Fig. 3. Effect of adrenomedullin on cell number in the adventitia (A) and collagen deposition/medial area (B). Values are means±S.E.M., (n). $^{**}P<0.01$ vs. intact artery with saline infusion; $^{\#\#}P<0.01$ vs. intact artery with adrenomedullin infusion; $^{++}P<0.01$ vs. injured artery with saline infusion.

but this reduction was statistically insignificant (Fig. 4A), and no significant differences were noted in the vessel area of four study groups (Fig. 4B). As shown in Fig. 4C, the ratio of the lumen to vessel area was significantly ($P<0.001$) reduced by the balloon injury in the saline group, compared with those of the intact arteries. The adrenomedullin supplement significantly ($P=0.030$) reversed this geometrical change toward those of the intact arteries.

4. Discussion

We report here that intravenous adrenomedullin infusion not only attenuated neointima formation but also inhibited fibroblast proliferation and collagen deposition of the adventitia, reducing the ratio of lumen to vessel area, in the balloon-injured carotid arteries of rats. The three layers of the vascular wall, intima, media and adventitia, contribute to inward or outward remodeling which occurs following arterial injury (Ward et al., 2000). Although neointimal formation and medial hypertrophy have been focused on as targets in preventing adverse remodeling, recent reports have

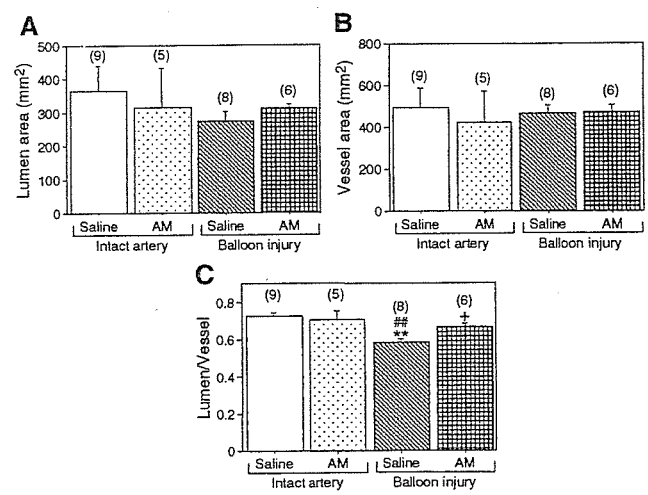

Fig. 4. Effect of adrenomedullin on lumen area (A), vessel area (B) and ratio of lumen to vessel area (C). Values are means±S.E.M., (n). $^{**}P<0.01$ vs. intact artery with saline infusion; $^{\#\#}P<0.01$ vs. intact artery with adrenomedullin infusion; $^{+}P<0.05$ vs. injured artery with saline infusion.

referred more to the role of the adventitial layer (Ryan et al., 2003; Sartore et al., 2001; Strauss and Rabinovitch, 2000).

In a model of arterial injury, endothelial denudation induces VSMC proliferation and migration, making up the neointima formation. Our present data supports previous studies showing that adrenomedullin attenuated the neointima formation induced by arterial injuries in rats (Agata et al., 2003; Yamasaki et al., 2003) and in mice (Imai et al., 2002; Kawai et al., 2004). On the other hand, extracellular matrix deposition in the adventitia with cellular hyperplasia appears to be the major phenomena responsible for adventitial thickening that would subsequently increase stiffness of the vascular walls and peripheral arterial resistance (Intengan and Schiffrin, 2001; Sartore et al., 2001). Importantly, we found that the adrenomedullin administration significantly decreased the number of fibroblasts in the adventitia following the arterial injury in this study. In addition, the adrenomedullin-treated rats showed a significant reduction of collagen deposition in the entire vessel wall, mainly in the adventitia. Considering the importance of extracellular matrix formation in determining stiffness of the vascular wall (Intengan and Schiffrin, 2001), adrenomedullin may exert a beneficial action alleviating vascular stiffness.

In this study, the beneficial effects of adrenomedullin following arterial injury were observed without a significant effect on blood pressure, suggesting a direct action of adrenomedullin on the vascular remodeling. Adrenomedullin has been shown to directly inhibit proliferation and migration of cultured VSMC (Kano et al., 1996; Kohno et al., 1997), and according to our previous report (Tsuruda et al., 1999), adrenomedullin inhibited proliferation of cultured fibroblasts isolated from rat cardiac ventricle. Recently, we reported that adrenomedullin induced matrix metalloproteinase-2 activity in cultured adventitial fibroblasts isolated from rat aorta (Tsuruda et al., 2004). Collagen accumulation is responsible for constrictive remodeling following balloon injury (Ryan et al., 2003). Proteolytic activity induced by adrenomedullin may have contributed to attenuating collagen deposition, however these hypotheses for possible, direct actions of adrenomedullin should be tested in vivo by future experiments.

In summary, the intravenous adrenomedullin infusion effectively improves the vascular geometry of the balloon-injured rat carotid artery, suppressing neointima formation, adventitial fibroblast proliferation and collagen deposition. This study implies a possible utility of adrenomedullin for inhibition of vascular remodeling, where both neointimal formation and adventitial hyperplasia are targeted.

Acknowledgements

This study was supported by the grants-in-aid for Scientific Research and for the 21st Century Centers of Excellence Program (Life Science) from the Ministry of Education, Culture, Sport, Science and Technology, Japan, and by a grant -in-aid from AstraZeneca Research 2003. We gratefully thank Ms. Ritsuko Sotomura for her technical assistance.

References

Agata, J., Zhang, J.J., Chao, J., Chao, L., 2003. Adrenomedullin gene delivery inhibits neointima formation in rat artery after balloon angioplasty. Regul. Pept. 112, 115–120.

De Meyer, G.R., Bult, H., 1997. Mechanisms of neointima formation—lessons from experimental models. Vasc. Med. 2, 179–189.

Imai, Y., Shindo, T., Maemura, K., Sata, M., Saito, Y., Kurihara, Y., Akishita, M., Osuga, J., Ishibashi, S., Tobe, K., Morita, H., Oh-hashi, Y., Suzuki, T., Maekawa, H., Kangawa, K., Minamino, N., Yazaki, Y., Nagai, R., Kurihara, H., 2002. Resistance to neointimal hyperplasia and fatty streak formation in mice with adrenomedullin overexpression. Arterioscler. Thromb. Vasc. Biol. 22, 1310–1315.

Intengan, H.D., Schiffrin, E.L., 2001. Vascular remodeling in hypertension. Roles of apoptosis, inflammation, and fibrosis. Hypertension 38, 581–587.

Kano, H., Kohno, M., Yasunari, K., Yokokawa, K., Horio, T., Ikeda, M., Minami, M., Hanehira, T., Takeda, T., Yoshikawa, J., 1996. Adrenomedullin as a novel antiproliferative factor of vascular smooth muscle cells. J. Hypertens. 14, 209–213.

Kawai, J., Ando, K., Tojo, A., Shimosawa, T., Takahashi, K., Onozato, M.L., Yamasaki, M., Ogita, T., Nakaoka, T., Fujita, T., 2004. Endogenous adrenomedullin protects against vascular response to injury in mice. Circulation 109, 1147–1153.

Kitamura, K., Kangawa, K., Kawamoto, M., Ichiki, Y., Nakamura, S., Matsuo, H., Eto, T., 1993. Adrenomedullin: a novel hypotensive peptide isolated from human pheochromocytoma. Biochem. Biophys. Res. Commun. 192, 553–560.

Kitamura, K., Kangawa, K., Eto, T., 2002. Adrenomedullin and PAMP: discovery, structures, and cardiovascular functions. Microsc. Res. Tech. 57, 3–13.

Kohno, M., Yokokawa, K., Kano, H., Yasunari, K., Minami, M., Hanehira, T., Yoshikawa, J., 1997. Adrenomedullin is a potent inhibitor of angiotensin II-induced migration of human coronary artery smooth muscle cells. Hypertension 29, 1309–1313.

Pasterkamp, G., Galis, Z.S., de Kleijn, D.P., 2004. Expansive arterial remodeling: location, location, location. Arterioscler. Thromb. Vasc. Biol. 24, 650–657.

Ryan, S.T., Koteliansky, V.E., Gotwals, P.J., Lindner, V., 2003. Transforming growth factor-beta-dependent events in vascular remodeling following arterial injury. J. Vasc. Res. 40, 37–46.

Sartore, S., Chiavegato, A., Faggin, E., Franch, R., Puato, M., Ausoni, S., Pauletto, P., 2001. Contribution of adventitial fibroblasts to neointima formation and vascular remodeling: from innocent bystander to active participant. Circ. Res. 89, 1111–1121.

Strauss, B.H., Rabinovitch, M., 2000. Adventitial fibroblasts: defining a role in vessel wall remodeling. Am. J. Respir. Cell Mol. Biol. 22, 1–3.

Tsuruda, T., Kato, J., Kitamura, K., Kawamoto, M., Kuwasako, K., Imamura, T., Koiwaya, Y., Tsuji, T., Kangawa, K., Eto, T., 1999. An autocrine or a paracrine role of adrenomedullin in modulating cardiac fibroblast growth. Cardiovasc. Res. 43, 958–967.

Tsuruda, T., Kato, J., Cao, Y.N., Hatakeyama, K., Masuyama, H., Imamura, T., Kitamura, K., Asada, Y., Eto, T., 2004. Adrenomedullin induces matrix metalloproteinase-2 activity in rat aortic adventitial fibroblasts. Biochem. Biophys. Res. Commun. 325, 80–84.

Yamasaki, M., Kawai, J., Nakaoka, T., Ogita, T., Tojo, A., Fujita, T., 2003. Adrenomedullin overexpression to inhibit cuff-induced arterial intimal formation. Hypertension 41, 302–307.

Ward, M.R., Pasterkamp, G., Yeung, A.C., Borst, C., 2000. Arterial remodeling. Mechanisms and clinical implications. Circulation 102, 1186–1191.

Adrenomedullin Enhances Angiogenic Potency of Bone Marrow Transplantation in a Rat Model of Hindlimb Ischemia

Takashi Iwase, MD; Noritoshi Nagaya, MD; Takafumi Fujii, MD; Takefumi Itoh, MD; Hatsue Ishibashi-Ueda, MD; Masakazu Yamagishi, MD; Kunio Miyatake, MD; Toshio Matsumoto, MD; Soichiro Kitamura, MD; Kenji Kangawa, PhD

Background—Previous studies have shown that adrenomedullin (AM) inhibits vascular endothelial cell apoptosis and induces angiogenesis. We investigated whether AM enhances bone marrow cell–induced angiogenesis.

Methods and Results—Immediately after hindlimb ischemia was created, rats were randomized to receive AM infusion plus bone marrow–derived mononuclear cell (MNC) transplantation (AM+MNC group), AM infusion alone (AM group), MNC transplantation alone (MNC group), or vehicle infusion (control group). The laser Doppler perfusion index was significantly higher in the AM and MNC groups than in the control group (0.74 ± 0.11 and 0.69 ± 0.07 versus 0.59 ± 0.07, respectively, $P<0.01$), which suggests the angiogenic potency of AM and MNC. Importantly, improvement in blood perfusion was marked in the AM+MNC group (0.84 ± 0.08). Capillary density was highest in the AM+MNC group, followed by the AM and MNC groups. In vitro, AM inhibited MNC apoptosis, promoted MNC adhesiveness to a human umbilical vein endothelial cell monolayer, and increased the number of MNC-derived endothelial progenitor cells. In vivo, AM administration not only enhanced the differentiation of MNC into endothelial cells but also produced mature vessels that included smooth muscle cells.

Conclusions—A combination of AM infusion and MNC transplantation caused significantly greater improvement in hindlimb ischemia than MNC transplantation alone. This effect may be mediated in part by the angiogenic potency of AM itself and the beneficial effects of AM on the survival, adhesion, and differentiation of transplanted MNCs. (***Circulation.* 2005;111:356-362.**)

Key Words: peptides ■ angiogenesis ■ peripheral vascular disease

Peripheral vascular disease is a crucial health issue that affects an estimated 27 million people.[1] Despite recent advances in medical intervention, the symptoms of some patients with critical limb ischemia fail to be controlled. Bone marrow–derived mononuclear cells (MNCs) include a variety of stem and progenitor cells, such as endothelial progenitor cells (EPCs), and contribute to pathological neovascularization.[2] MNC transplantation induces therapeutic angiogenesis in ischemic limb[3,4]; however, some patients fail to respond to this cell therapy. Thus, a novel therapeutic strategy to enhance the angiogenic property of MNCs is desirable.

Adrenomedullin (AM) is a potent vasodilator peptide that was originally isolated from human pheochromocytoma.[5] Previous studies have reported that abnormalities of vascular structure are present in homozygous AM knockout mice.[6,7] A recent study has demonstrated that blood flow recovery in ischemic limb and tumor angiogenesis are substantially impaired in heterozygous AM knockout mice.[8] Furthermore, AM has been shown to inhibit vascular endothelial cell apoptosis and induce angiogenesis through the activation of the phosphatidylinositol 3-kinase (PI3K)/Akt pathway.[9,10] These results suggest that AM is indispensable for modulating angiogenesis and vasculogenesis. When these findings are taken together, combination therapy with MNC transplantation and AM infusion may have additional or synergetic effects on therapeutic angiogenesis for the treatment of severe peripheral vascular disease. Thus, the purposes of the present study were (1) to investigate whether local infusion of AM enhances the angiogenic potency of MNC transplantation in a rat model of hindlimb ischemia and (2) to investigate the effects of AM on the survival, adhesion, and differentiation of transplanted MNCs.

Received June 18, 2004; revision received September 9, 2004; accepted November 3, 2004.

From the Departments of Regenerative Medicine and Tissue Engineering (T. Iwase, N.N., T. Itoh), Cardiac Physiology (T.F.), and Biochemistry (K.K.), National Cardiovascular Center Research Institute, Osaka, Japan; Departments of Internal Medicine (N.N., M.Y., K.M.), Pathology (H.I.-U.), and Cardiovascular Surgery (S.K.), National Cardiovascular Center, Osaka, Japan; and Department of Medicine and Bioregulatory Sciences (T. Iwase, T.M.), University of Tokushima Graduate School of Medicine, Tokushima, Japan.

Reprint requests to Noritoshi Nagaya, MD, Department of Regenerative Medicine and Tissue Engineering, National Cardiovascular Center Research Institute, 5-7-1 Fujishirodai, Suita, Osaka 565-8565, Japan. E-mail nagayann@hsp.ncvc.go.jp

Circulation is available at http://www.circulationaha.org

DOI: 10.1161/01.CIR.0000153352.29335.B9

Methods

Animal Model of Hindlimb Ischemia

Male Lewis rats (weight 250 to 275 g; Japan SLC Inc, Hamamatsu, Japan) were used in the present study. The left common iliac artery of each rat was resected under anesthesia with pentobarbital sodium (50 mg/kg). The distal portion of the saphenous artery and all side branches and veins were dissected free and excised. The right hindlimb was kept intact and used as the nonischemic limb. Transplantation of bone marrow–derived MNCs and infusion of AM were performed in 40 rats immediately after hindlimb ischemia was created. This protocol resulted in the creation of 4 groups: (1) AM infusion plus MNC transplantation (AM+MNC group, n=10), (2) AM infusion plus PBS injection (AM group, n=10), (3) vehicle infusion plus MNC transplantation (MNC group, n=10), and (4) vehicle infusion plus PBS injection (control group, n=10). The Animal Care Committee of the National Cardiovascular Center approved this experimental protocol.

MNC Transplantation and AM Infusion

Bone marrow was harvested from the femur and tibia in other male Lewis rats, and MNCs were isolated by Ficoll density gradient centrifugation (Lymphoprep, Nycomed). MNCs (5×10^6 cells per animal) or PBS was injected into the ischemic thigh muscle with a 26-gauge needle at 5 different points. Human recombinant AM (0.01 $\mu g \cdot kg^{-1} \cdot min^{-1}$) or vehicle was administered for 7 days with a mini-osmotic pump (ALZET, Palo Alto) implanted in the left inguinal region.

Assessment of Blood Perfusion

To measure serial blood flow for 3 weeks, we used a laser Doppler perfusion image (LDPI) analyzer (Moor Instrument). After blood flow was scanned twice, the average flow values of the ischemic and nonischemic limbs were calculated by computer-assisted quantification. The LDPI index was determined as the ratio of ischemic to nonischemic hindlimb blood perfusion.[11]

Histological Assessment

Three weeks after MNC transplantation and/or AM infusion, 4 pieces of ischemic tissue from the adductor and semimembranous muscles were obtained and snap-frozen in liquid nitrogen. Frozen tissue sections were stained with alkaline phosphatase by an indoxyl tetrazolium method to detect capillary endothelial cells.[3,11] Five fields were randomly selected to count the number of capillaries. The capillary number adjusted per muscle fiber was used to compare the differences in capillary density among the 4 groups.[3]

Monitoring of Transplanted MNCs in Ischemic Hindlimb Muscle

To examine differentiation of transplanted MNCs, 5×10^6 MNCs labeled with red fluorescent dye (PKH26-GL, Sigma Chemical Co) were transplanted into the ischemic thigh muscle in rats with (n=3) and without (n=3) AM infusion. Three weeks after transplantation, frozen tissue sections from ischemic muscle were incubated with anti-von Willebrand factor antibody (vWF, DAKO), anti-CD31 antibody (BD Pharmingen), and anti-α-smooth muscle actin antibody (α-SMA, DAKO), followed by incubation with Alexa Fluor 633 IgG antibody (Molecular Probes) and FITC-conjugated IgG antibody (BD Pharmingen), respectively. Five high-power fields (40×) of each section were randomly selected to count the number of transplanted MNCs, vWF-positive cells, and α-SMA–positive cells.

In Situ Detection of MNC Apoptosis

PKH26-labeled MNCs (5×10^6 cells per animal) were transplanted into the ischemic muscle in rats with (n=2) and without (n=2) AM infusion. Twenty-four hours after transplantation, apoptosis of transplanted MNCs in ischemic tissue was evaluated by terminal dUTP nick-end labeling (TUNEL) assay (ApopTag Fluorescein kit, Serological Corporation), as reported previously.[12]

In Vitro Apoptosis Assay

The antiapoptotic effect of AM on MNCs was evaluated by TUNEL assay. Human MNCs, isolated from peripheral blood, were plated on 12-well plates (1×10^6 cells per well) and cultured in serum-free medium for 24 hours with control buffer, AM, or AM plus wortmannin, a PI3K inhibitor (50 nmol/L). TUNEL for detection of apoptotic nuclei was performed according to the manufacturer's instructions. MNCs were then mounted in medium that contained 4′,6-diamidino-2-phenylindole (DAPI). Randomly selected microscopic fields (n=10) were evaluated to calculate the ratio of TUNEL-positive cells to total cells.

Adhesion Assay

We evaluated whether AM enhances MNC adhesiveness according to a previously reported method.[13] In brief, human umbilical vein endothelial cells (HUVECs) were cultured to confluence on 6-well plates with or without pretreatment with tumor necrosis factor-α (1 ng/mL). In the absence or presence of AM (10^{-7} mol/L), 1×10^6 MNCs labeled with PKH26 were incubated on an HUVEC monolayer for 24 hours. Nonadherent MNCs were removed, and the number of PKH26-positive cells in each well was counted.

Cell ELISA

Expression of adhesion molecules in HUVECs was measured by cell ELISA, as reported previously.[14] In brief, confluent HUVECs on 96-well plates were treated with AM (10^{-7} mol/L) or control buffer for 4 hours. HUVECs were then incubated with monoclonal mouse antibodies against intercellular adhesion molecule-1 (ICAM-1, R&D Systems) and vascular adhesion molecule-1 (VCAM-1, R&D Systems). A protein detector ELISA kit (KPL) was used to detect bound monoclonal antibodies.

EPC Culture Assay

Culture of EPCs was performed as described previously.[11,15,16] In brief, 2×10^6 MNCs were plated in Medium-199 supplemented with 20% FCS, heparin, and antibiotics on fibronectin-coated 6-well plates. AM (10^{-7} mol/L), human recombinant vascular endothelial growth factor (VEGF; 20 ng/mL), or control buffer was added to each plate. After 7 days of culture, nonadherent cells were removed, and adherent cells were incubated with acetylated LDL labeled with DiI (DiI-acLDL, Biomedical Technologies) and FITC-labeled lectin from ulex europaeus (Sigma). Double-positive cells for DiI-acLDL and FITC-labeled lectin were identified as EPCs.[16] Randomly selected microscopic fields (n=10) were evaluated to count the number of EPCs.

Fluorescence-Activated Cell Sorting Analysis

Fluorescence-activated cell sorting was performed to identify characteristics of adherent cells after 7 days of culture.[16] Cells were incubated for 30 minutes at 4°C with anti-human CD31 antibodies (clone L133.1, Becton Dickinson), anti-human KDR antibodies (clone KDR-1, Sigma), and anti-human VE-cadherin antibodies (clone BV6, Chemicon). Isotype-identical antibodies served as controls. Fluorescence-activated cell sorting analyses were performed with a FACSCalibur flow cytometer and Cell Quest software (BD Biosciences).

Real-Time Polymerase Chain Reaction

Expression of calcitonin receptor-like receptor (CRLR), a receptor for AM, was examined by real-time polymerase chain reaction (PCR). Total RNA was extracted from MNCs, EPCs, and HUVECs with an RNA extraction kit (RNeasy Mini Kit, Qiagen) and converted to cDNA by reverse transcription. Real-time PCR was performed with SYBR green dye (QuantiTect SYBR Green PCR kit, Qiagen) and a Prism 7700 sequence detection system (Applied Biosystems). The PCR primers for CRLR were as follows: sense primer 5′-CATTCAACAAGCAGAAGGCG-3′ and antisense primer 5′-AGCCATCCATCCCAGGTTC-3′. For GAPDH, the primers were as follows: sense primer 5′-CAATGCCTCCTGCACCACCAA-3′ and antisense primer 5′-GAGGCAGGGATGATGTTCTGGA-3′. Levels of CRLR mRNA were normalized to that of

GAPDH mRNA. PCR-amplified products were also electrophoresed on 2% agarose gels to confirm that single bands were amplified.

In Vitro Matrigel Assay

HUVECs (1×10^5 cells) were seeded onto 24-well plates coated with Matrigel (Becton Dickinson) in the presence of the combination of control buffer, AM (10^{-7} mol/L), VEGF (10 ng/mL), or neutralizing antibodies against KDR (2 μg/mL, R&D Systems). After incubation for 18 hours, tube formation area was measured as described previously.[17] The control was defined as 100% tube formation, and the percent increase was calculated for each sample.

Measurements of Cytokines

A total of 1×10^6 MNCs or HUVECs were plated in serum-free medium with or without AM (10^{-7} mol/L) on 12-well plates. After 24-hour incubation, the conditioned medium was collected, and VEGF, basic fibroblast growth factor, and hepatocyte growth factor were measured with enzyme immunoassay kits (R&D Systems).

Migration Assay

Migration assay of smooth muscle cells (SMCs) was performed with Transwell (Coster) 24-well plates composed of a collagen-coated membrane with 8-μm pores. Human aortic SMCs, preincubated with serum-free medium for 24 hours to maintain quiescence, were seeded on the upper chamber at a concentration of 1×10^6 cells/mL. Serum-free medium containing control buffer, AM (10^{-7} mol/L), or AM plus wortmannin (50 nmol/L) was placed in the lower chamber. After incubation for 12 hours, the number of migrated cells was counted in the randomly selected fields (n=5).

Statistical Analysis

All values are expressed as mean±SEM. Student's unpaired *t* test was used to compare differences between 2 groups. Comparisons of parameters among 3 or 4 groups were made by 1-way ANOVA, followed by Scheffé multiple comparison test. Comparisons of the time course of the LDPI index were made by 2-way ANOVA for repeated measures, followed by Scheffé multiple comparison tests. A probability value <0.05 was considered statistically significant.

Results

Blood Perfusion and Capillary Density

Blood perfusion of the ischemic hindlimb increased modestly but gradually in the AM and MNC groups after treatment (Figure 1A). Interestingly, blood perfusion in the AM+MNC group markedly improved within 2 weeks after treatment and showed further improvement thereafter. The LDPI index was significantly higher in the AM, MNC, and AM+MNC groups than in the control group 3 weeks after surgery (Figure 1B). Importantly, the LDPI index was highest in the AM+MNC group among the 4 groups.

Alkaline phosphatase staining of ischemic muscle showed significant augmentation of neovascularization in the AM, MNC, and AM+MNC groups (Figure 2A). The capillary/muscle fiber ratio of ischemic muscle was highest in the AM+MNC group, followed by the MNC group, AM group, and control group (Figure 2B).

Differentiation of Transplanted MNCs

Three weeks after MNC transplantation, PKH26-labeled MNCs were frequently observed in the AM+MNC group, and these transplanted cells were positive for vWF (Figure 3A). Most of these cells were also stained by CD31 (data not shown). The number of PKH26/vWF double-positive cells was significantly higher in the AM+MNC group than in the MNC group (Figure 3B). Although PKH26/α-SMA double-positive cells were not detected in ischemic muscle of each group, newly formed vascular structures in the AM+MNC group included α-SMA–positive cells (Figure 3C). The number of α-SMA–positive cells in the MNC-derived vascular structures was significantly higher in the AM+MNC group than in the MNC group (Figure 3D).

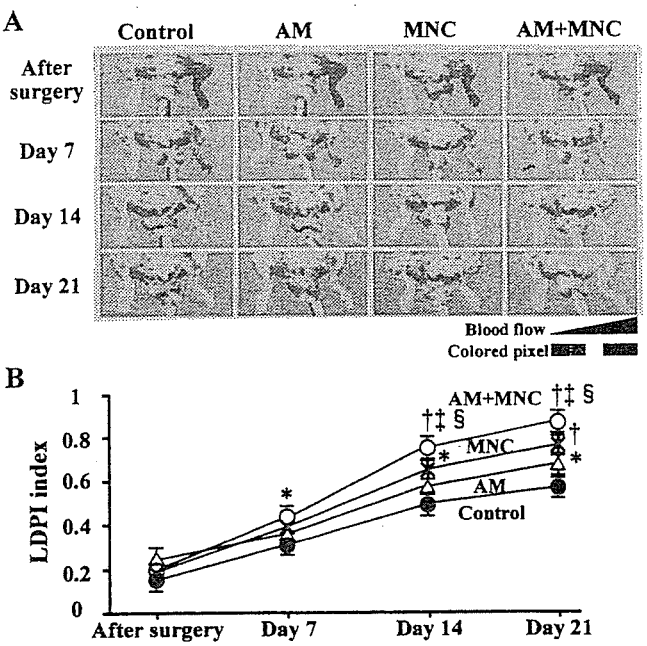

Figure 1. A, Representative examples of serial laser Doppler perfusion images. Blood perfusion of ischemic hindlimb increased notably in AM+MNC group (red to yellow). B, Quantitative analysis of hindlimb blood perfusion with LDPI index, ratio of ischemic to nonischemic hindlimb blood perfusion. Data are mean±SEM. **P*<0.05 and †*P*<0.01 vs control; ‡*P*<0.01 vs AM; §*P*<0.05 vs MNC.

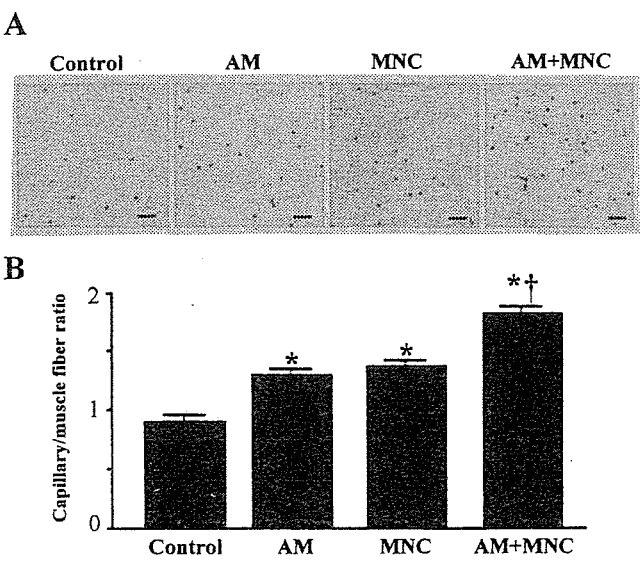

Figure 2. A, Representative photographs of alkaline phosphatase staining in ischemic hindlimb muscles. Capillary density in AM+MNC group was markedly higher than that in other groups. B, Quantitative analysis of capillary density in ischemic hindlimb muscles. Data are mean±SEM. **P*<0.01 vs control; †*P*<0.01 vs AM and MNC. Scale bars: 50 μm.

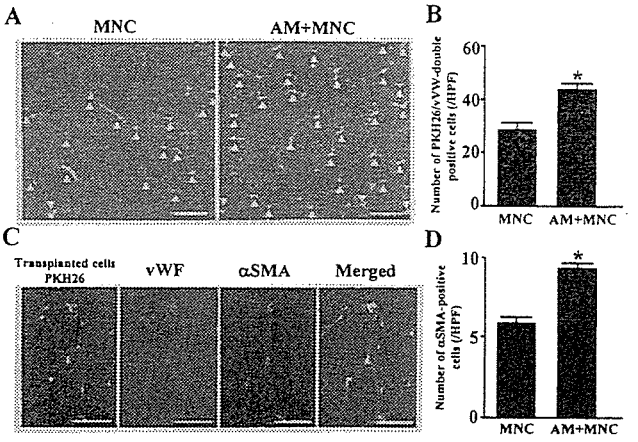

Figure 3. In vivo differentiation of transplanted MNCs. A, Representative photographs of MNC-derived vascular structures in MNC and AM+MNC groups. Red fluorescence (PKH26)–labeled MNCs were transplanted into ischemic thigh muscle. PKH26 (red)/vWF (blue) double-positive cells (pink, arrows) were frequently observed in AM+MNC group. B, Number of PKH26/vWF double-positive cells (MNC-derived endothelial cells) was significantly higher in AM+MNC group than in MNC group. C, Representative photographs of newly formed mature vessels in AM+MNC group. MNC-derived vascular structures often included α-SMA–positive cells (green). D, Number of α-SMA–positive cells in MNC-derived vessels was significantly higher in AM+MNC group than in MNC group. Data are mean±SEM. *$P<0.01$ vs MNC. Bars: 50 μm. HPF indicates high-power field.

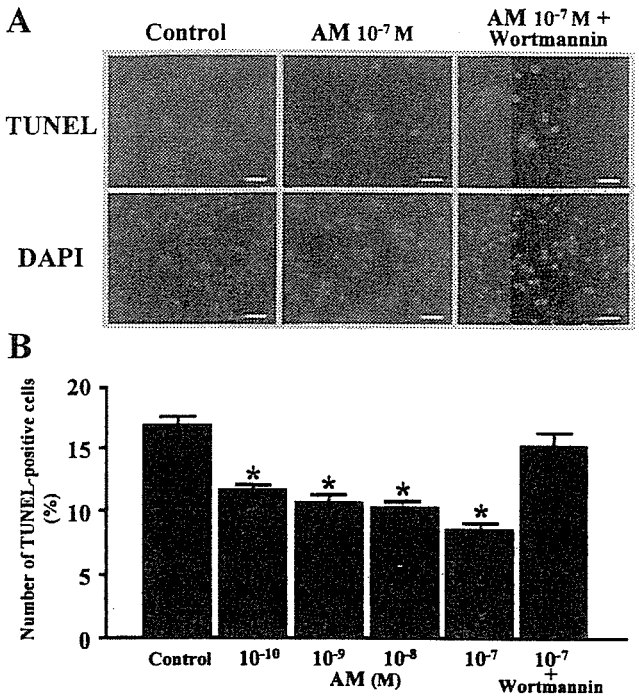

Figure 4. Apoptosis assay. A, Apoptosis of MNC was detected by TUNEL assay (green). Nuclei of MNC were stained with DAPI (blue). AM inhibited MNC apoptosis in serum-free medium. B, Quantitative analysis. AM decreased percentage of TUNEL-positive cells in dose-dependent manner. Pretreatment with wortmannin, a PI3K inhibitor, diminished antiapoptotic effect of AM. Data are mean±SEM. *$P<0.01$ vs control. Bars: 50 μm.

Antiapoptotic Effect of AM on MNCs

In vitro, serum starvation induced MNC apoptosis, as indicated by detection of TUNEL-positive cells (Figure 4A). When incubated in the presence of AM, the percentage of TUNEL-positive cells markedly decreased in a dose-dependent manner (Figure 4B). However, pretreatment with wortmannin, a PI3K inhibitor, diminished the antiapoptotic effect of AM. Similarly, in vivo, local administration of AM decreased TUNEL-positive MNC 24 hours after transplantation (data not shown).

Effect of AM on MNC Adhesiveness

The number of adherent MNCs on an HUVEC monolayer increased significantly in the presence of AM (10^{-7} mol/L) compared with control (Figures 5A and 5B). With pretreatment using tumor necrosis factor-α, AM also enhanced the adhesiveness of MNCs to HUVECs. AM significantly enhanced expression of ICAM-1 and VCAM-1 in HUVECs (Figure 5C).

Effect of AM on EPC Expansion

After 7-day culture of human MNCs, spindle-shaped or cobblestone-like adherent cells were observed (Figure 6A). Most of the adherent cells were double stained with DiI-acLDL and FITC-labeled lectin. These adherent cells expressed endothelial cell–specific markers: KDR, VE cadherin, and CD31 (Figure 6B). Thus, we identified the major population of the adherent cells as EPCs. Culture of MNCs with AM significantly increased the number of EPCs (Figure 6C). The effect of AM was equivalent to that of VEGF. Real-time PCR revealed that MNCs, EPCs, and HUVECs expressed mRNA of CRLR (Figure 6D). Expression of CRLR mRNA was highest in HUVECs, followed by EPCs and MNCs.

Effects of AM on Tube Formation and SMC Migration

Like VEGF, AM induced tube formation in HUVECs in vitro (Figure 7A). Blocking antibodies against KDR significantly inhibited VEGF-induced tube formation, whereas they did not suppress AM-induced tube formation (Figure 7B). AM did not significantly alter VEGF, basic fibroblast growth factor, or hepatocyte growth factor levels in conditioned medium of cultured MNCs or HUVECs (data not shown). AM significantly increased the number of migrated SMCs compared with control (Figures 7C and 7D). Pretreatment with wortmannin diminished the effect of AM on SMC migration.

Discussion

In the present study, we demonstrated in vivo that AM infusion or MNC transplantation alone induced angiogenesis in a rat model of hindlimb ischemia, the combination of AM infusion and MNC transplantation enhanced MNC-induced angiogenesis, and AM increased the number of MNC-derived vWF-positive cells and generated α-SMA–positive vascular structures. We also demonstrated in vitro that AM inhibited serum starvation–induced MNC apoptosis, promoted MNC adhesiveness to an HUVEC monolayer, increased the number of MNC-derived EPCs, and stimulated SMC migration.

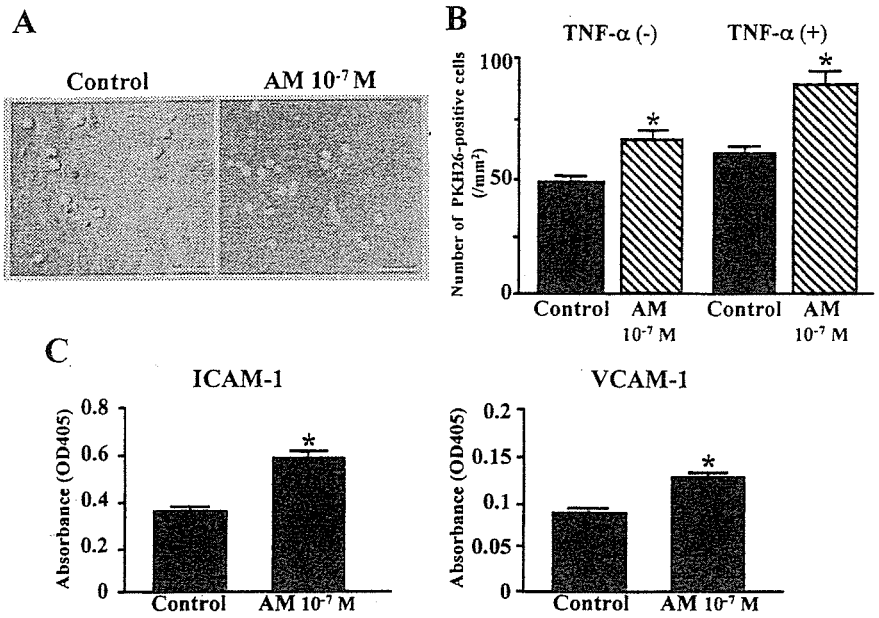

Figure 5. A and B, Adhesion assay. Representative photographs of red fluorescence–labeled MNC adhesion to HUVEC monolayer with and without AM (A). Quantitative analysis of MNC adhesion (B). Bars: 50 μm. C, Surface expression of ICAM-1 and VCAM-1 in HUVECs with or without AM. Data are mean±SEM. TNF indicates tumor necrosis factor. *$P<0.01$ vs control.

MNC transplantation causes therapeutic angiogenesis by supplying EPCs and multiple angiogenic cytokines such as VEGF.[3,4] The present study showed that local infusion of AM significantly increased blood perfusion and capillary density in ischemic hindlimb muscle. Furthermore, a combination of AM infusion and MNC transplantation significantly increased blood perfusion and capillary density of the ischemic hindlimb compared with MNC transplantation alone. AM has been shown to induce angiogenesis in vitro and in vivo through the PI3K/Akt pathway.[10,18] In the present study, AM-induced tube formation was not blocked by neutralizing antibodies against KDR. In addition, AM did not enhance VEGF secretion from MNCs and HUVECs. Thus, beneficial effects of combination therapy

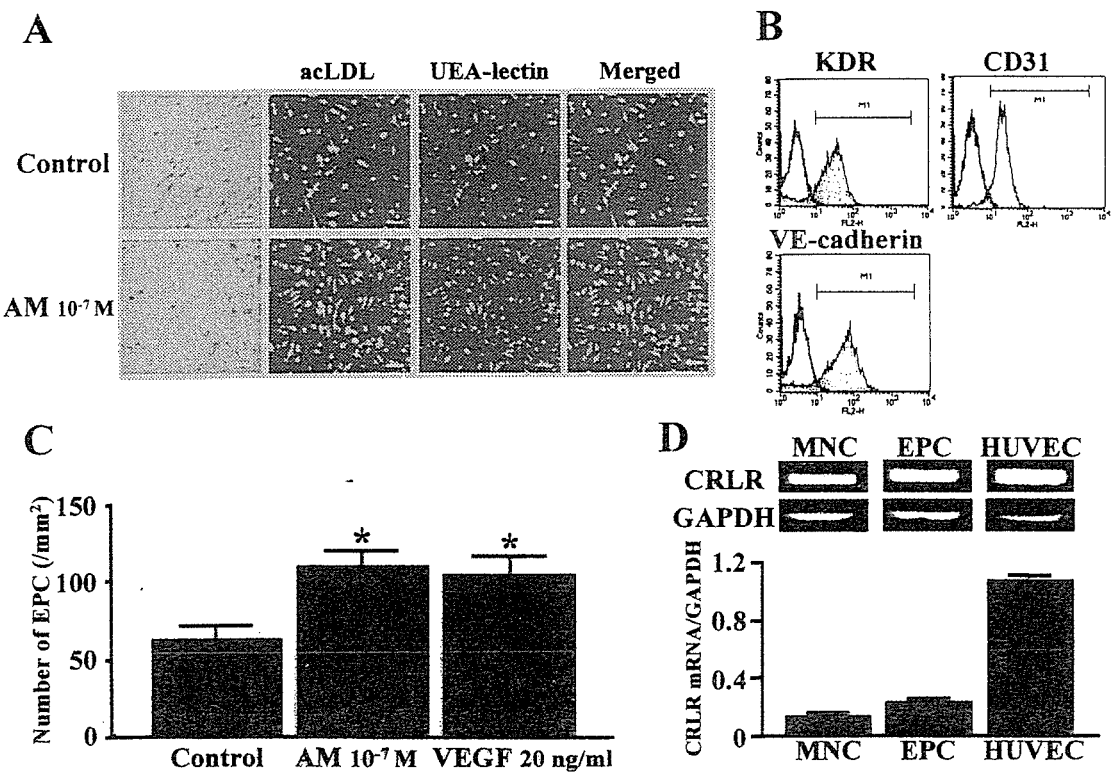

Figure 6. A through C, EPC culture assay. Cultured adherent cells took up DiI-acLDL (red) and FITC-labeled lectin (green) in same fields (A). Fluorescence-activated cell sorting analyses revealed that most adherent cells expressed KDR, VE cadherin, and CD31 (B). Culture of MNCs with AM significantly increased number of EPCs. Effect of AM was equivalent to that of VEGF (C). Data are mean±SEM. *$P<0.01$ vs control. Bars: 50 μm. D, Quantitative analysis of AM receptor (CRLR) mRNA expression in MNCs, EPCs, and HUVECs. UEA indicates ulex europaeus.

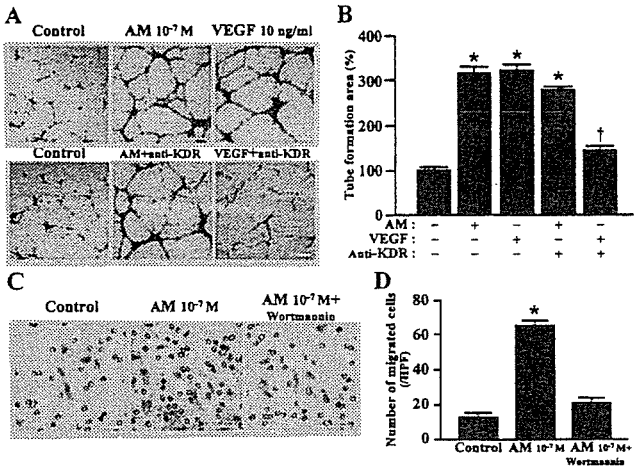

Figure 7. A and B, Matrigel assay. Representative photographs of tube formation (A). Quantitative analysis of tube formation area (B). Data are mean±SEM. *$P<0.01$ vs control; †$P<0.01$ vs VEGF. Bars: 20 μm. C and D, Migration assay. Representative photographs of migrated SMCs (C). Quantitative analyses of SMC migration (D). Data are mean±SEM. *$P<0.01$ vs control. Bars: 50 μm.

with AM and MNCs may be attributable in part to the angiogenic properties of AM itself.

An earlier study has shown that transplanted MNCs disappear from ischemic muscle 7 days after transplantation.[19] We demonstrated that apoptosis of MNCs occurred in ischemic muscle 24 hours after MNC transplantation. These results raise the possibility that the angiogenic potency of MNC transplantation is attenuated by MNC apoptosis. In the present study, AM inhibited apoptosis of MNCs in vitro and in vivo, and the antiapoptotic effect of AM was suppressed by wortmannin, a PI3K inhibitor. These findings suggest that AM prolongs MNC survival through the PI3K/Akt pathway and thereby enhances neovascularization in ischemic tissue.

In the present study, AM promoted adhesiveness of MNCs to an HUVEC monolayer. AM significantly enhanced expression of ICAM-1 and VCAM-1 in HUVECs, both of which facilitate adhesion of MNCs to endothelial cells.[20] These findings suggest that AM increases MNC adhesiveness to endothelial cells via activation of adhesion molecules. A recent study has shown that MNC adhesiveness to endothelial cells is indispensable for MNC differentiation into endothelial lineage.[21] Thus, it is possible that AM infusion enhances the angiogenic potency of MNCs at least in part through promotion of adhesion of MNC to host vascular endothelial cells.

VEGF has been shown to increase the number of EPCs in vitro and in vivo, resulting in angiogenesis and vasculogenesis.[13,22] The present study showed that MNCs and EPCs expressed CRLR, a receptor of AM. In vitro, AM increased the number of MNC-derived EPCs that expressed VE cadherin, KDR, and CD31. The effect of AM on EPC expansion was equivalent to that of VEGF. In vivo, AM infusion increased the number of MNC-derived vWF-positive cells, although incorporation of these cells in the capillaries may be due in part to incorporation of hematopoietic cells. These findings suggest that AM may accelerate MNC differentiation into endothelial lineage.

SMC is essential for the generation of functional and mature blood vessels.[23] We demonstrated in vivo that local infusion of AM increased the number of α-SMA–positive cells (SMCs) in MNC-derived vascular structures. In vitro, AM enhanced SMC migration, which was inhibited by wortmannin, a PI3K inhibitor. Recent studies using homozygous AM knockout mice have suggested that AM is indispensable for vascular morphogenesis.[6,7] When these findings are taken together, it is possible that AM contributes to vessel maturation through enhancement of SMC migration via the PI3K/Akt-dependent pathway.

Currently, a new therapeutic approach to augment the efficacy of MNC transplantation is awaited for the treatment of severe peripheral vascular disease. The present study demonstrated that local infusion of AM enhanced the angiogenic potency of MNC transplantation. In the present study, AM inhibited MNC apoptosis and increased the total number of engrafted cells in ischemic tissue, although this study did not show the effect of AM on specific cell populations of MNCs. In addition, AM promoted cell proliferation, migration, and differentiation. We have already demonstrated the safety of AM infusion in patients with congestive heart failure.[24] Thus, combination therapy with AM infusion and MNC transplantation may be a novel and promising therapeutic strategy for the treatment of severe peripheral vascular disease.

Conclusions

A combination of AM infusion and MNC transplantation caused significantly greater improvement in hindlimb ischemia than MNC transplantation alone. This effect may be mediated in part by the angiogenic potency of AM itself and the beneficial effects of AM on the survival, adhesion, and differentiation of transplanted MNCs.

Acknowledgments

This work was supported by the research grant for cardiovascular disease (16C-6) from the Ministry of Health, Labor and Welfare, Industrial Technology Research Grant Program in '03 from New Energy and Industrial Technology Development Organization (NEDO) of Japan, Health and Labor Sciences Research Grants-genome 005, the Mochida Memorial Foundation for Medical and Pharmaceutical Research, and the Promotion of Fundamental Studies in Health Science of the Organization for Pharmaceutical Safety and Research (OPSR) of Japan.

References

1. Belch JJ, Topol EJ, Agnelli G, et al. Critical issues in peripheral arterial disease detection and management: a call to action. *Arch Intern Med.* 2003;163:884–892.
2. Asahara T, Masuda H, Takahashi T, et al. Bone marrow origin of endothelial progenitor cells responsible for postnatal vasculogenesis in physiological and pathological neovascularization. *Circ Res.* 1999;85:221–228.
3. Shintani S, Murohara T, Ikeda H, et al. Augmentation of postnatal neovascularization with autologous bone marrow transplantation. *Circulation.* 2001;103:897–903.
4. Tateishi-Yuyama E, Matsubara H, Murohara T, et al. Therapeutic angiogenesis for patients with limb ischaemia by autologous transplantation of bone-marrow cells: a pilot study and a randomised controlled trial. *Lancet.* 2002;360:427–435.

5. Kitamura K, Kangawa K, Kawamoto M, et al. Adrenomedullin: a novel hypotensive peptide isolated from human pheochromocytoma. *Biochem Biophys Res Commun.* 1993;192:553–560.
6. Shindo T, Kurihara Y, Nishimatsu H, et al. Vascular abnormalities and elevated blood pressure in mice lacking adrenomedullin gene. *Circulation.* 2001;104:1964–1971.
7. Caron KM, Smithies O. Extreme hydrops fetalis and cardiovascular abnormalities in mice lacking a functional adrenomedullin gene. *Proc Natl Acad Sci U S A.* 2001;98:615–619.
8. Iimuro S, Shindo T, Moriyama N, et al. Angiogenic effects of adrenomedullin in ischemia and tumor growth. *Circ Res.* 2004;95: 415–423.
9. Kim W, Moon SO, Sung MJ, et al. Protective effect of adrenomedullin in mannitol-induced apoptosis. *Apoptosis.* 2002;7:527–535.
10. Miyashita K, Itoh H, Sawada N, et al. Adrenomedullin provokes endothelial Akt activation and promotes vascular regeneration both in vitro and in vivo. *FEBS Lett.* 2003;544:86–92.
11. Murohara T, Ikeda H, Duan J, et al. Transplanted cord blood-derived endothelial precursor cells augment postnatal neovascularization. *J Clin Invest.* 2000;105:1527–1536.
12. Okumura H, Nagaya N, Itoh T, et al. Adrenomedullin infusion attenuates myocardial ischemia/reperfusion injury through the phosphatidylinositol 3-kinase/Akt-dependent pathway. *Circulation.* 2004;109:242–248.
13. Iwaguro H, Yamaguchi J, Kalka C, et al. Endothelial progenitor cell vascular endothelial growth factor gene transfer for vascular regeneration. *Circulation.* 2002;105:732–738.
14. Byrne MF, Corcoran PA, Atherton JC, et al. Stimulation of adhesion molecule expression by Helicobacter pylori and increased neutrophil adhesion to human umbilical vein endothelial cells. *FEBS Lett.* 2002;532: 411–414.
15. Asahara T, Murohara T, Sullivan A, et al. Isolation of putative progenitor endothelial cells for angiogenesis. *Science.* 1997;275:964–967.
16. Nagaya N, Kangawa K, Kanda M, et al. Hybrid cell-gene therapy for pulmonary hypertension based on phagocytosing action of endothelial progenitor cells. *Circulation.* 2003;108:889–895.
17. Miura S, Matsuo Y, Saku K. Transactivation of KDR/Flk-1 by the B2 receptor induces tube formation in human coronary endothelial cells. *Hypertension.* 2003;41:1118–1123.
18. Tokunaga N, Nagaya N, Shirai M, et al. Adrenomedullin gene transfer induces therapeutic angiogenesis in a rabbit model of chronic hindlimb ischemia: benefits of a novel nonviral vector, gelatin. *Circulation.* 2004; 109:526–531.
19. Iba O, Matsubara H, Nozawa Y, et al. Angiogenesis by implantation of peripheral blood mononuclear cells and platelets into ischemic limbs. *Circulation.* 2002;106:2019–2025.
20. Peled A, Grabovsky V, Habler L, et al. The chemokine SDF-1 stimulates integrin-mediated arrest of CD34(+) cells on vascular endothelium under shear flow. *J Clin Invest.* 1999;104:1199–1211.
21. Fujiyama S, Amano K, Uehira K, et al. Bone marrow monocyte lineage cells adhere on injured endothelium in a monocyte chemoattractant protein-1-dependent manner and accelerate reendothelialization as endothelial progenitor cells. *Circ Res.* 2003;93:980–989.
22. Asahara T, Takahashi T, Masuda H, et al. VEGF contributes to postnatal neovascularization by mobilizing bone marrow-derived endothelial progenitor cells. *EMBO J.* 1999;18:3964–3972.
23. Rissanen TT, Markkanen JE, Gruchala M, et al. VEGF-D is the strongest angiogenic and lymphangiogenic effector among VEGFs delivered into skeletal muscle via adenoviruses. *Circ Res.* 2003;92:1098–1106.
24. Nagaya N, Satoh T, Nishikimi T, et al. Hemodynamic, renal, and hormonal effects of adrenomedullin infusion in patients with congestive heart failure. *Circulation.* 2000;101:498–503.

Adrenomedullin Enhances Therapeutic Potency of Mesenchymal Stem Cells After Experimental Stroke in Rats

Kenichiro Hanabusa, MD; Noritoshi Nagaya, MD; Takashi Iwase, MD; Takefumi Itoh, MD; Shinsuke Murakami, MD; Yoshito Shimizu, MD; Waro Taki, MD; Kunio Miyatake, MD; Kenji Kangawa, PhD

Background and Purpose—Adrenomedullin (AM) induces angiogenesis and inhibits cell apoptosis through the phosphatidylinositol 3-kinase/Akt pathway. Transplantation of mesenchymal stem cells (MSCs) has been shown to improve neurological deficits after stroke in rats. We investigated whether AM enhances the therapeutic potency of MSC transplantation.

Methods—Male Lewis rats (n=100) were subjected to 2-hour middle cerebral artery occlusion. Immediately after reperfusion, rats were assigned randomly to receive intravenous transplantation of MSCs plus subcutaneous infusion of AM for 7 days (MSC+AM group), AM infusion alone (AM group), MSC transplantation alone (MSC group), or vehicle infusion (control group). Neurological and immunohistological assessments were performed to examine the effects of these treatments.

Results—Some engrafted MSCs were positive for neuronal and endothelial cell markers, although the number of differentiated MSCs did not differ significantly between the MSC and MSC+AM groups. The neurological score significantly improved in the MSC, AM, and MSC+AM groups compared with the control group. Importantly, improvement in the MSC+AM group was significantly greater than that in the MSC and AM groups. There was marked induction of angiogenesis in the ischemic penumbra in the MSC+AM group, followed by the AM, MSC, and control groups. AM infusion significantly inhibited apoptosis of transplanted MSCs. As a result, the number of engrafted MSCs in the MSC+AM group was significantly higher than that in the MSC group.

Conclusions—AM enhanced the therapeutic potency of MSCs, including neurological improvement, possibly through inhibition of MSC apoptosis and induction of angiogenesis. (***Stroke*. 2005;36:853-858.)**

Key Words: angiogenesis ■ apoptosis ■ stroke

Despite the advances in medical and surgical treatment, stroke is still a major cause of morbidity and mortality. Mesenchymal stem cells (MSCs) are multipotent, and some transplanted MSCs can differentiate into neuronal cells and endothelial cells in the recipient brain.[1] A recent study has shown that MSCs have ability to pass blood–brain barrier, particularly in injury sites.[1–3] In addition, transplantation of MSCs into the brain of experimental stroke animals has been shown to improve neurological functional recovery.[1,3] The effect of MSC transplantation is dependent on the number of transplanted MSCs.[1] However, the viability of MSCs after transplantation is relatively poor.[4] Thus, a new approach to augment the effect of MSC transplantation is desirable for the application of MSC therapy to the regenerative treatment of stroke.

Adrenomedullin (AM) is a potent vasodilatory peptide that was originally isolated from human pheochromocytoma.[5] Recent study has shown that intramuscular administration of AM DNA induces therapeutic angiogenesis in a hindlimb ischemic model via activation of Akt.[6] In addition, AM has been shown to exert antiapoptotic effects on a variety of cells.[7] We also demonstrated antiapoptotic effects of AM in myocardial ischemia/reperfusion injury through the phosphatidylinositol 3-kinase (PI3K)/Akt pathway.[8] These results suggest that AM may play an important role in induction of angiogenesis and inhibition of apoptosis. Taking these findings together, AM infusion may have additive or synergetic effects on MSC transplantation, which may result in improvement of neurological functional recovery. Thus, the purpose of this study was to investigate whether combined therapy of AM infusion and MSC transplantation significantly improves neurological functional recovery compared with MSC transplantation alone.

Received December 7, 2004; accepted January 6, 2005.

From the Department of Regenerative Medicine and Tissue Engineering (K.H., N.N., T. Iwase, T. Itoh, S.M., Y.S.), National Cardiovascular Center Research Institute, Osaka, Japan; Department of Neurosurgery (K.H., W.T.), Mie University School of Medicine, Mie, Japan; Department of Internal Medicine (K.M.), National Cardiovascular Center, Osaka, Japan; and Department of Biochemistry (K.K.), National Cardiovascular Center Research Institute, Osaka, Japan.

Reprint requests to Noritoshi Nagaya, MD, Department of Regenerative Medicine and Tissue Engineering, National Cardiovascular Center Research Institute, 5-7-1 Fujishirodai, Suita, Osaka 565-8565, Japan. E-mail nnagaya@ri.ncvc.go.jp

Stroke is available at http://www.strokeaha.org

DOI: 10.1161/01.STR.0000157661.69482.76

Materials and Methods

Stroke Model

Male Lewis rats (Japan SLC, Hamamatsu, Japan) weighing 230 to 260 g were used in all experiments. Middle cerebral artery occlusion (MCAO) was performed by an intraluminal thread as described previously.[2] The animal care committee of the National Cardiovascular Center approved this experimental protocol.

MSC Preparation

MSC expansion was performed according to a previously described method.[9] In brief, we euthanized male Lewis rats and harvested bone marrow. Bone marrow cells were introduced into 100-mm dishes and cultured in α-minimum essential medium (MEN) supplemented with 10% FBS. After nonadherent hematopoietic cells were removed with medium replacement, spindle-shaped adherent cells developed visible symmetric colonies by day 5 to 7. They were expanded to >50 million cells, ≈4 to 5 passages. These adherent cells were collected with 0.05% trypsin and 2% EDTA (GIBCO) for 3 minutes at 37°C. These cells were analyzed by fluorescence-activated cell sorting as described previously.[10] Most of cultured adherent cells were positive for CD29 (98±1%) and CD90 (99±1%) and negative for CD34 (2±1%) and CD45 (1±1%). We confirmed that major population of the adherent cells were MSCs. MSCs secreted a large amount of an antiapoptotic and angiogenic factor, including vascular endothelial growth factor (VEGF; 960±14 pg/10^6 cells), 24 hours after culture.

MSC Transplantation and AM Infusion

Immediately after 2-hour MCAO, rats were assigned randomly to the following 4 groups. (1) PBS injection plus vehicle infusion (control group n=22); (2) MSC injection plus vehicle infusion (MSC group n=28); (3) PBS injection and AM infusion (AM group n=22); and (4) MSC injection plus AM infusion (MSC+AM group n=28). MSCs (1×10^6 cells) suspended in PBS were injected via a tail vein. Four rats underwent a sham operation without an intraluminal thread. AM (0.05 μg/kg per minute) or vehicle was infused for 7 days using a mini-osmotic pump (Alzet) implanted in the posterior cervical subcutaneous region. The dose of AM used in this study has antiapoptotic effects without significant hypotension.[8]

Detection of MSC Differentiation in Ischemic Hemisphere

Red fluorescent-labeled MSCs were transplanted to examine MSC differentiation as described previously.[11] In brief, suspended MSCs were labeled with fluorescent dye (PKH26 Red Fluorescent Cell Linker Kit; Sigma). Three minutes after labeling, FBS was added for 1 minute to stop reaction and cells were washed by PBS. A recent study has shown that the sensitivity and specificity for cell labeling with PKH26 are ≈100%, and transplanted cells are detectable at least up to 4 months after transplantation in the host brain.[11] Rats were euthanized with an overdose of pentobarbital on day 14 after MCAO. For preparation of frozen sections, rats were perfused transcardially with normal saline and the brain was removed immediately. Blocks corresponding to coronal coordinates for bregma −1 to 1 mm were obtained and frozen rapidly in liquid nitrogen. A series of 6-μm-thick sections was obtained. Numbers of PKH26-positive cells were counted in a blind fashion and expressed as the average in 5 sections. To detect the differentiation of MSCs, immunohistochemical staining was performed. Sections were incubated with anti-von Willebrand factor (vWF) polyclonal antibody (1:200; DAKO, Glostrup, Denmark), rabbit anti-glial fibrillary acidic protein (GFAP; 1:500; DAKO), and mouse anti-neuronal nuclei marker (NeuN; 1:200; Chemicon, Hampshire, UK), followed by incubation with fluorescein isothiocynate (FITC)–conjugated rabbit immunoglobulin antibody (DAKO) and FITC-conjugated mouse immunoglobulin antibody (BD Pharmingen, San Diego, Calif), respectively.

Neurological Assessment

Neurological assessment was performed on days 1, 7, and 14 using a modified neurological severity score, as described previously.[1] In brief, this score is derived by evaluating animals for hemiparesis (response to raising the rat by the tail or placing the rat on a flat surface), sensory deficits (placing, proprioception), beam balance tests (response to placement and posture on a narrow beam and time before dropping), absent reflexes (pinna, corneal, startle), and abnormal movement (seizure, myoclonus, myodystony). One point is awarded for the inability to perform a task or for the lack of a tested reflex.

Measurement of Infarct Size

Rats were euthanized on day 1 (each group n=8) and on day 14 (each group n=8). For preparation of paraffin-embedded sections, rats were perfused transcardially with 4% paraformaldehyde. Brains were cut into 7 equally spaced (2 mm) coronal blocks, and each section was stained with hematoxylin and eosin. Infarct size was determined by the "indirect method," as described previously,[1] and expressed as a percentage of the intact contralateral hemispheric size.

Assessment of Angiogenesis

Angiogenesis was analyzed on day 14 (each group n=8). Paraffin sections corresponding to coronal coordinates for bregma −1 to 1 mm were selected. Sections were incubated with anti-vWF antibody and then incubated with biotinylated anti-rabbit immunoglobulin and with streptoavidin-horseradish peroxidase (HRP) complex (DAKO). The HRP reaction was detected in diaminobenzidine (DAB). To quantify angiogenesis, 8 fields of view from the ischemic penumbra and contralateral noninfarct tissue were randomly selected as described previously,[2] and images (×100 magnification) were acquired using a microscope (ZWISS AXIOVERT 135) and a digital camera (ZWISS AXIO cam). The vWF-immunoreactive area in each image was determined by image analysis using software (Win Roof 5.0; Microsoft) as described previously.[12] The values corresponding to total brown areas were averaged and expressed as the mean percentage of stained vessel area per 100 μm^2. To detect newly formed vessels, tissue sections were stained for Ki67, a marker for cell proliferation, with the use of monoclonal anti-Ki67 antibody (DAKO). The numbers of Ki67-positive microvessels were counted and expressed the average in 8 fields.

Detection of Apoptosis in Ischemic Penumbra

The antiapoptotic effects of AM on the ischemic penumbra were examined 24 hours after MCAO (each group n=8). Paraffin-embedded sections were prepared for TUNEL assay. TUNEL staining was performed with a commercially available kit (ApopTag Plus; Serological Corporation). The numbers of TUNEL-positive cells per field were counted and expressed as the average in 8 fields. To evaluate apoptosis of transplanted MSCs in the ischemic brain, an additional 12 rats (MSC group n=6; MSC+AM group n=6) were euthanized on day 3. Frozen sections were used for TUNEL staining (ApopTag Fluorescein kit). The numbers of TUNEL- and PKH26-positive cells were counted and expressed as the average in 5 sections.

Statistical Analysis

All data were expressed as mean±SEM. Student's unpaired t test was used to compare differences between 2 groups. Comparisons of parameters among 4 groups were made by 1-way ANOVA, followed by Newman–Keuls test. Comparisons of the time course of neurological scores were made by 2-way ANOVA for repeated measures, followed by Newman–Keuls test. A P value <0.05 was considered statistically significant.

Results

Engraftment and Differentiation of Transplanted MSCs

Intravenously administered MSCs were engrafted in the ischemic penumbra. Some MSCs were positive for NeuNs and GFAP (Figure 1A and 1B). Other MSCs were positive for

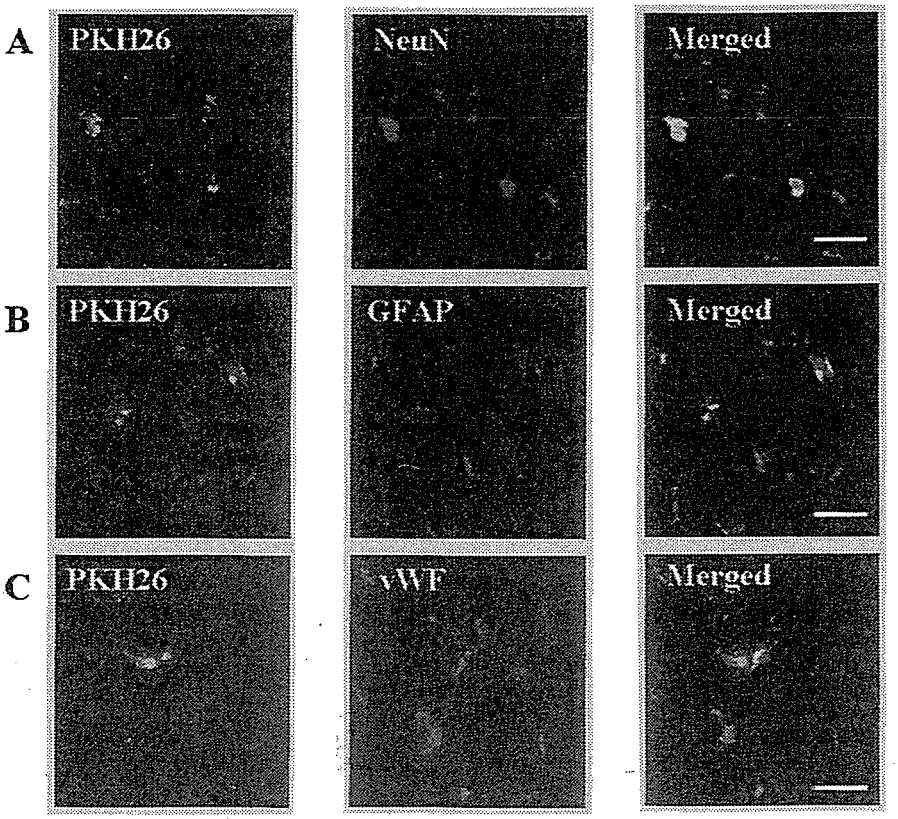

Figure 1. Engraftment and differentiation of transplanted MSCs. PKH26-labeled MSCs were frequently observed in ischemic penumbra. Some PKH26-positive MSCs (red) expressed neuronal marker (NeuN; green; A), astrocyte marker (GFAP; green; B), or endothelial cell marker (vWF; green; C). Bars=20 μm.

vascular endothelial marker vWF (Figure 1C). The numbers of differentiated MSCs did not differ significantly between the MSC and MSC+AM groups (data not shown). Few MSCs were observed in the contralateral nonischemic tissue.

Neurological Assessment

Neurological severity scores on day 1 did not differ significantly among 4 groups (Figure 2). Neurological deficits gradually improved in all groups. Scores in the MSC and AM groups on days 7 and 14 were lower than those in the control group ($P<0.05$), although there were no significant differences between the AM and MSC groups on days 7 and 14. Interestingly, the scores on days 7 and 14 were lowest in the MSC+AM group among the 4 groups.

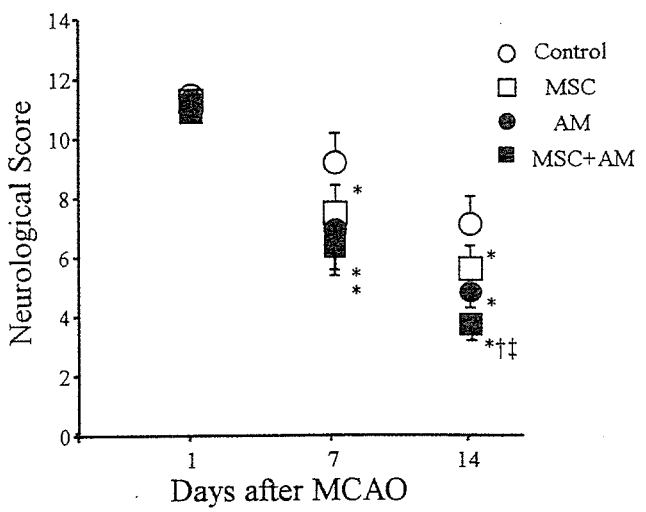

Figure 2. Neurological score on days 1, 7, and 14 in the control group, MSC group, AM group, and MSC+AM group. Data are mean±SEM. *$P<0.05$ vs control group; †$P<0.05$ vs MSC group; ‡$P<0.05$ vs AM group.

Infarct Size and Physiological Data

Infarct size on day 1 in the MSC or AM group was significantly smaller than that in the control group ($P<0.05$; Table 1). Furthermore, the infarct size in the MSC+AM group was the smallest among 4 groups. However, on day 14, there was no significant difference in infarct size, although the infarct size tended to be small in the treatment groups. Percent increase in body weight in the MSC, AM, and MSC+AM groups was higher than that in the control group ($P<0.05$; Table 2).

TABLE 1. Percent Infarct Size to the Contralateral Hemisphere

		Infarct Size (%)	
Group	No.	Day 1	Day 14
Control	8	31±1	31±2
MSC	8	27±1*	29±2
AM	8	28±1*	29±1
MSC+AM	8	25±1*†‡	28±2

Control indicates rats given vehicle infusion; MSC, rats given MSC transplantation; AM, rats given AM infusion; MSC+AM, rats given MSC transplantation and AM infusion.

Data are mean±SEM.

*$P<0.05$ vs control group.

†$P<0.05$ vs MSC group.

‡$P<0.05$ vs AM group.

TABLE 2. Percent Increase of Body Weight

Group	No.	% Increase of Body Weight
Control	16	8±3
MSC	16	12±2*
AM	16	13±2*
MSC+AM	16	14±2*

Control indicates rats given vehicle infusion; MSC, rats given MSC transplantation; AM, rats given AM infusion; MSC+AM, rats given MSC transplantation and AM infusion.

Data are mean±SEM.

*$P<0.05$ vs control group.

Angiogenic Potency of AM and MSCs

Angiogenesis in the ischemic penumbra was observed after MCAO compared with sham operation (Figure 3A). Furthermore, MSC transplantation or AM infusion induced angiogenesis in the ischemic penumbra, and particularly, the angiogenic effect was marked after combined therapy of MSCs and AM. Quantitative analysis demonstrated that the area of vWF staining in the MSC and AM groups was higher than that in the control group ($P<0.05$ versus control group; Figure 3B). There was no significant difference between the MSC and AM groups. Interestingly, the area of vWF staining in the MSC+AM group was highest among the 4 groups ($P<0.05$ versus MSC and AM groups). There were no significant differences in neovascularization of noninfarct tissue in all groups (Figure 3A and 3B). Representative photomicrographs of immunostaining of Ki67, a marker for cell proliferation, demonstrated that AM infusion and MSC transplantation increased the number of Ki67-positive newly formed microvessels in the ischemic penumbra (Figure 3C and 3D).

Antiapoptotic Effects of AM on Neuronal Cells and Transplanted MSCs

TUNEL-positive cells were frequently observed in the ischemic penumbra on day 1 (Figure 4A). Quantitative analysis demonstrated that the number of TUNEL-positive cells in the treatment groups was lower than that in the control group ($P<0.05$ versus control group; Figure 4B). Interestingly, the number of TUNEL-positive cells in the MSC+AM group was significantly lower than that in the MSC and AM groups ($P<0.05$ versus MSC and AM groups), although there was no significant difference between the MSC and AM groups.

The majority of transplanted MSCs were positive for TUNEL staining on day 3 (Figure 5A). Infusion of AM decreased TUNEL-positive MSCs in the ischemic penumbra. Quantitative analysis demonstrated that the number of apoptotic MSCs in the MSC+AM group was significantly lower than that in the MSC group ($P<0.05$; Figure 5B). As a result, the number of engrafted MSCs in the MSC+AM group on day 14 was markedly higher than that in the MSC group ($P<0.05$; Figure 5C). The number of TUNEL-positive non-

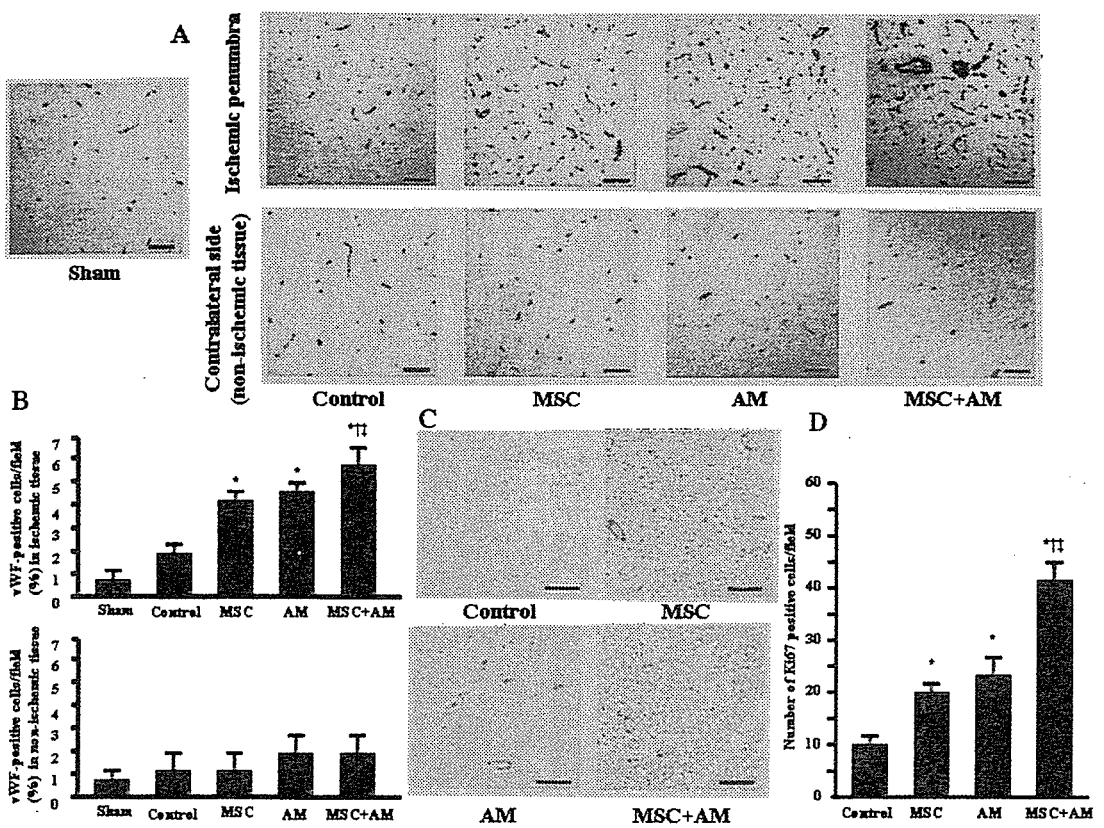

Figure 3. A, Representative photomicrographs of vWF staining in ischemic penumbra (top) and in contralateral nonischemic tissue (bottom). Bars=25 μm. B, Quantitative analysis of angiogenesis using the area of vWF staining in ischemic penumbra (top) and in nonischemic tissue (bottom). C, Representative photomicrographs of Ki67 staining. Bars=50 μm. D, Quantitative analysis of the number of Ki67-positive microvessels. Data are mean±SEM. *$P<0.05$ vs control group; †$P<0.05$ vs MSC group; ‡$P<0.05$ vs AM group.

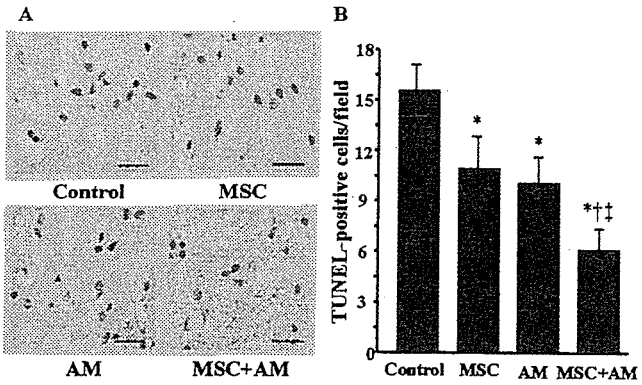

Figure 4. A, Representative photomicrographs of TUNEL staining in ischemic penumbra. The number of TUNEL-positive cells (DAB; brown) in the MSC+AM group was markedly lower than that in the other 3 groups. B, Quantitative analysis of the number of TUNEL-positive cells. Data are mean±SEM. *$P<0.05$ vs control group; †$P<0.05$ vs MSC group; ‡$P<0.05$ vs AM group. Bars=20 μm.

MSCs, including neuronal cells, was also decreased by AM infusion (Figure 5D).

Discussion

In the present study, we demonstrated that: (1) AM infusion or MSC transplantation induced angiogenesis and inhibited apoptosis of neuronal cells in the ischemic penumbra; (2) infusion of AM enhanced the angiogenic potency and antiapoptotic effects of MSC transplantation; (3) AM inhibited apoptosis of transplanted MSCs themselves and increased the number of engrafted MSCs; and (4) combination therapy of AM and MSC induced greater improvement in neurological functions than AM infusion or MSC transplantation alone.

Endogenous AM has been shown to be upregulated by hypoxia in the ischemic brain through a compensatory mechanism.[13] A previous report has demonstrated that pretreatment with AM reduces brain injury and improves neurological deficits in a rat stroke model.[14] The present study demonstrated that AM infusion after the onset of stroke improved neurological functions in rats. However, the underlying mechanisms still remain unclear. We have shown that intramuscular administration of AM DNA induces therapeutic angiogenesis in a hindlimb ischemic model via activation of Akt.[6] Expectedly, in the present study, infusion of AM induced neovascularization in the ischemic penumbra. On the other hand, AM has been shown to have potent antiapoptotic effects on various cells through the PI3K/Akt pathway.[7,8] Interestingly, in the present study, short-term infusion of AM markedly decreased TUNEL-positive cells in the ischemic penumbra. AM infusion significantly decreased infarct size on day 1, although the significant change was not observed on day 14. These results suggest that AM improves neurological functions, at least in part, through induction of angiogenesis and inhibition of neuronal cell apoptosis in the ischemic penumbra.

Recently, transplantation of MSCs has been shown to improve neurological functions in experimental stroke.[1,3] The beneficial effects are considered to be mediated by increases in endogenous angiogenic and antiapoptotic factors including VEGF, a potent neuroprotective factor,[12] and by differentiation of MSCs themselves into neuronal cells.[1] The present study showed that MSCs secreted a large amount of VEGF. In fact, we demonstrated in vivo that MSCs induced angiogenesis and inhibited cell apoptosis in the ischemic penumbra (Figures 3 and 4). Furthermore, some transplanted MSCs differentiated into neuronal cells and endothelial cells. Thus, MSCs have neuroprotective effects not only through their differentiation, but also through their ability to secret angiogenic and antiapoptotic factors. Nevertheless, the majority of transplanted MSCs were positive for TUNEL staining on day 3. Interestingly, infusion of AM significantly decreased the

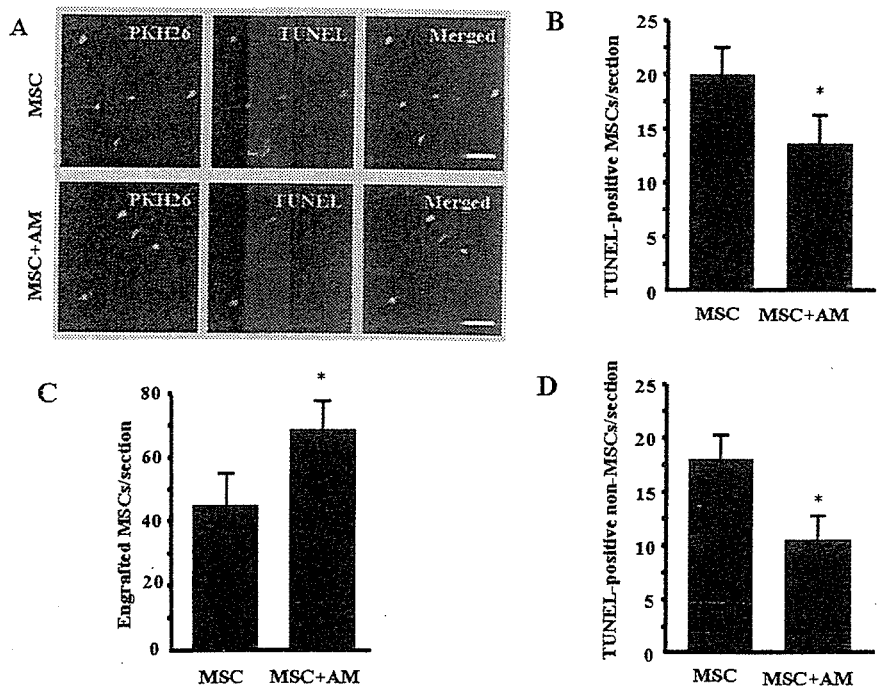

Figure 5. A, Representative photomicrographs of MSC apoptosis after transplantation. Transplanted MSCs were labeled with PKH26. TUNEL-positive cells (green) were frequently observed in ischemic penumbra. Infusion of AM decreased TUNEL-positive MSCs (double-positive cells, merged). B, Quantitative analysis of the number of TUNEL-positive MSCs on day 3. C, The number of engrafted MSCs on day 14. D, Quantitative analysis of the number of TUNEL-positive non-MSCs. Data are mean±SEM. *$P<0.05$. Bars=100 μm.